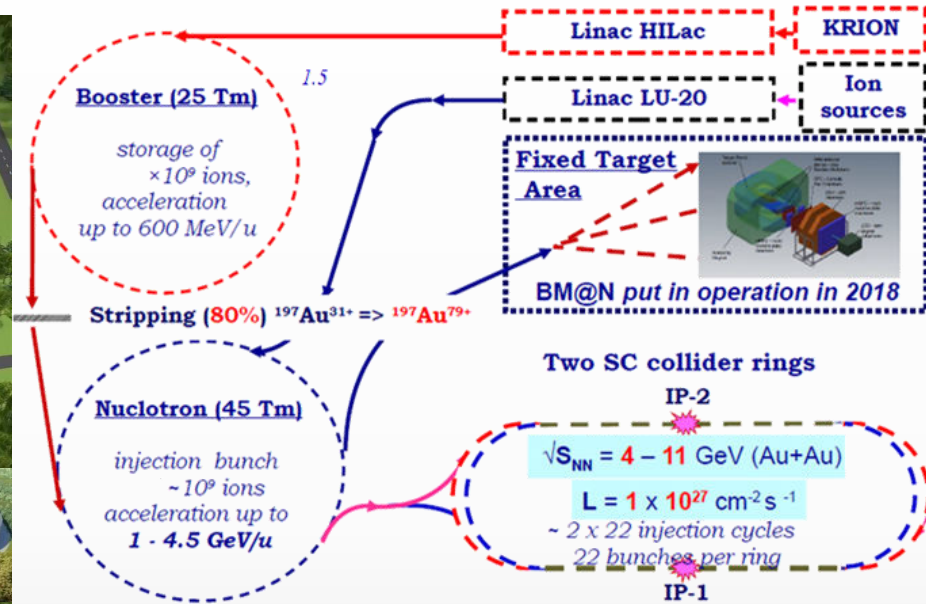


MPD physics program and its potential for first physics measurements

V. Riabov for the MPD Collaboration





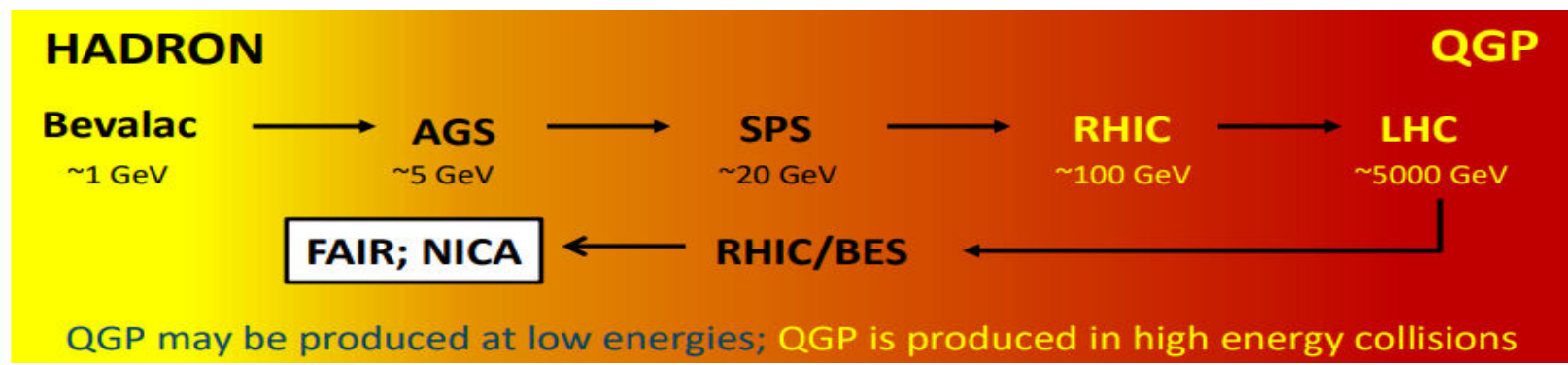
❖ The first megascience project in Russia, which is approaching its full commissioning:

- ✓ already running in the fixed-target mode – BM@N
- ✓ start of operation in collider mode in 2023-2024 – MPD and later SPD

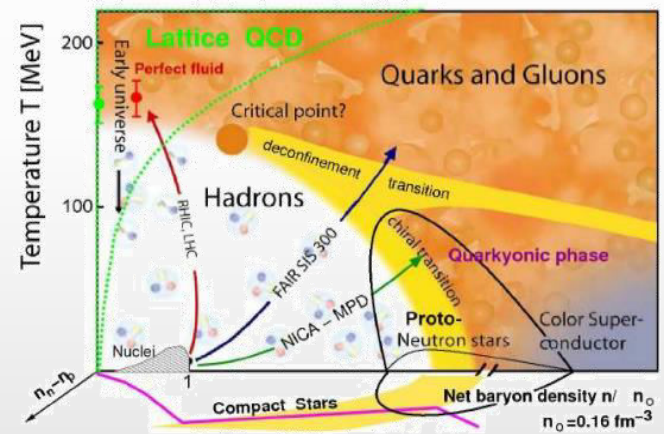
❖ Expected beam configuration in Stage-I:

- ✓ not-optimal beam optics with wide z-vertex distribution, $\sigma_z \sim 50 \text{ cm}$
- ✓ reduced luminosity ($\sim 10^{25}$) → collision rate $\sim 50 \text{ Hz}$
- ✓ collision system available with the current sources: C (A=12), N (A=14), Ar (A=40), Fe (A=56), Kr (A=78-86), Xe (A=124-134), Bi (A=209) → start with Bi+Bi @ 9.2 GeV in 2023-2024

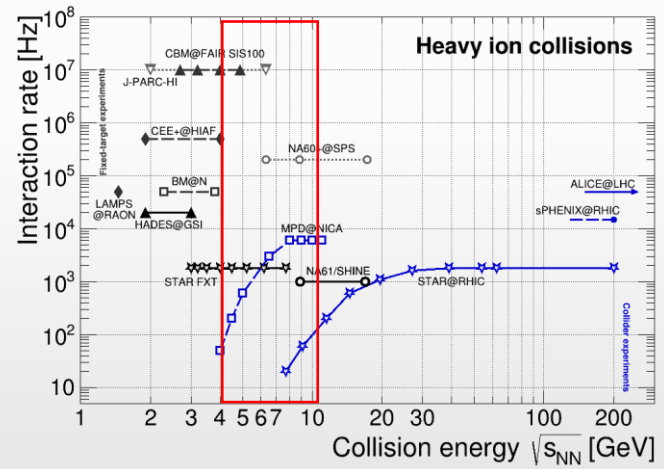
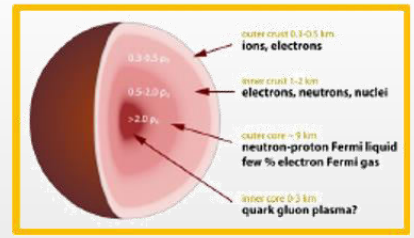
Heavy-ion collisions



https://github.com/tgalatyuk/interaction_rate_facilities



high baryon densities
→ inner structure of compact stars



- ❖ At $\mu_B \sim 0$, smooth crossover (lattice QCD calculations + data)
- ❖ At large μ_B , 1st order phase transition is expected → QCD critical point
- ❖ At NICA, both BM@N and MPD study QCD medium at extreme net baryon densities
- ❖ Many ongoing (HADES, NA61/Shine, STAR-BES) and future experiments in ~ same energy range

❖ Data taking by STAR at RHIC: $3 < \sqrt{s_{NN}} < 200$ GeV ($750 < \mu_B < 25$ MeV)

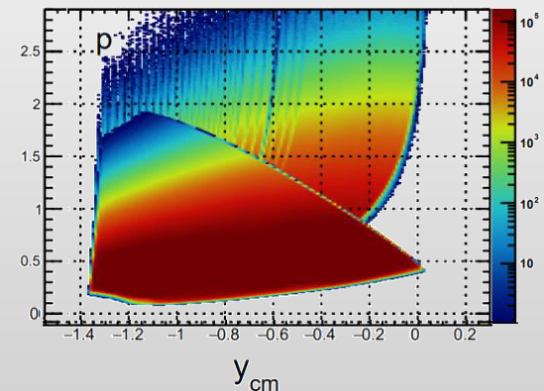
Au+Au Collisions at RHIC											
Collider Runs						Fixed-Target Runs					
	$\sqrt{s_{NN}}$ (GeV)	#Events	μ_B	y_{beam}	run		$\sqrt{s_{NN}}$ (GeV)	#Events	μ_B	y_{beam}	run
1	200	380 M	25 MeV	5.3	Run-10, 19	1	13.7 (100)	50 M	280 MeV	-2.69	Run-21
2	62.4	46 M	75 MeV		Run-10	2	11.5 (70)	50 M	320 MeV	-2.51	Run-21
3	54.4	1200 M	85 MeV		Run-17	3	9.2 (44.5)	50 M	370 MeV	-2.28	Run-21
4	39	86 M	112 MeV		Run-10	4	7.7 (31.2)	260 M	420 MeV	-2.1	Run-18, 19, 20
5	27	585 M	156 MeV	3.36	Run-11, 18	5	7.2 (26.5)	470 M	440 MeV	-2.02	Run-18, 20
6	19.6	595 M	206 MeV	3.1	Run-11, 19	6	6.2 (19.5)	120 M	490 MeV	1.87	Run-20
7	17.3	256 M	230 MeV		Run-21	7	5.2 (13.5)	100 M	540 MeV	-1.68	Run-20
8	14.6	340 M	262 MeV		Run-14, 19	8	4.5 (9.8)	110 M	590 MeV	-1.52	Run-20
9	11.5	157 M	316 MeV		Run-10, 20	9	3.9 (7.3)	120 M	633 MeV	-1.37	Run-20
10	9.2	160 M	372 MeV		Run-10, 20	10	3.5 (5.75)	120 M	670 MeV	-1.2	Run-20
11	7.7	104 M	420 MeV		Run-21	11	3.2 (4.59)	200 M	699 MeV	-1.13	Run-19
						12	3.0 (3.85)	2000 M	750 MeV	-1.05	Run-18, 21

❖ A very impressive and successful program with many collected datasets, already available and expected results

❖ Limitations:

- ✓ Au+Au collisions only
- ✓ Among the fixed-target runs, only the 3 GeV data have full mid-rapidity coverage for protons ($|y| < 0.5$), which is crucial for physics observables

Au+Au @ 3.9 GeV



- ❖ MPD strategy – high-luminosity scans in energy and system size to measure a wide variety of signals:
 - ✓ order of the phase transition and search for the QCD critical point → structure of the QCD phase diagram
 - ✓ hypernuclei and equation of state at high baryon densities → inner structure of compact stars, star mergers

- ❖ Scans to be carried out using the same apparatus in the same configuration/geometry with all the advantages of collider experiments:
 - ✓ maximum phase space, minimally biased acceptance, free of target parasitic effects
 - ✓ correlated systematic effects for different systems and energies → search for non-monotonic behavior of signals

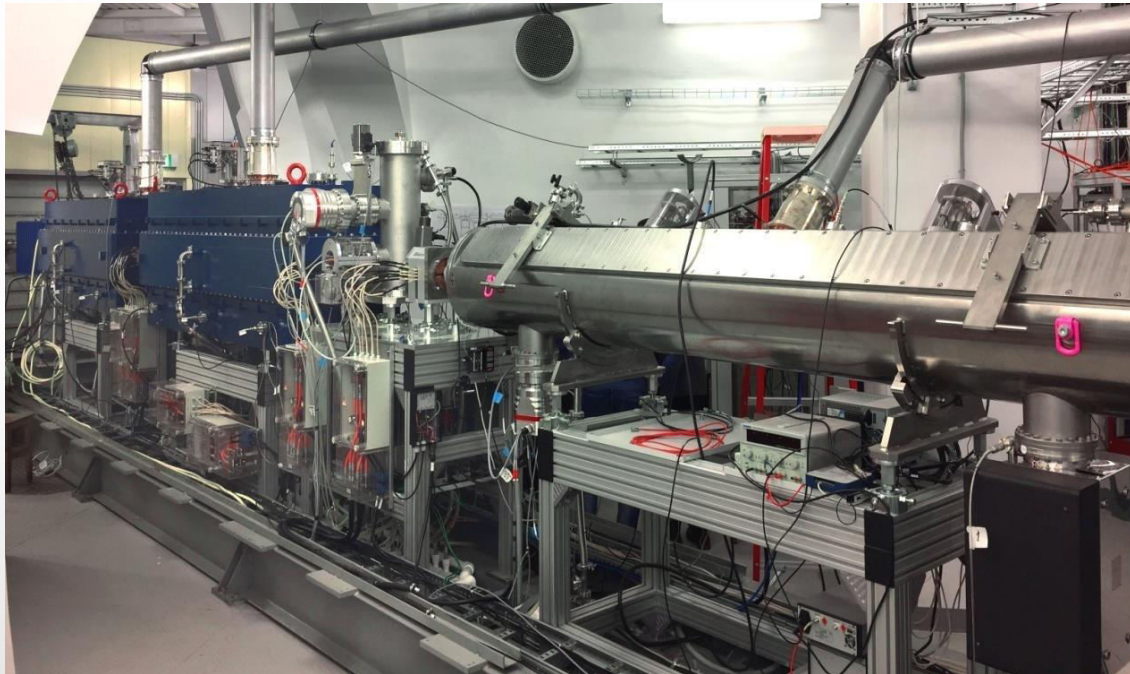
- ❖ Continuously develop physical program based on the recent advancements in the field:
 - ✓ identified particle spectra and ratios, collective flow and femtoscopy, production of strangeness and hypernuclei net-proton fluctuations, global polarization of hyperons and spin alignment of vector mesons, dilepton continuum and LVMs, etc.

- ❖ Work in close cooperation with theoreticians to look for new signals/observables including those unique for the MPD

Physical programs of the MPD ($\sqrt{s_{NN}} = 4-11$ GeV) and BM@N ($\sqrt{s_{NN}} = 2.3-3.5$ GeV) are bound and should be realized in close cooperation

❖ Stages of the accelerator complex commissioning

- ✓ HILAC + transfer line to Booster → commissioned in 2018 with He^{1+} , Fe^{14+} , C^{4+} , Ar^{14+} and Xe^{28+}

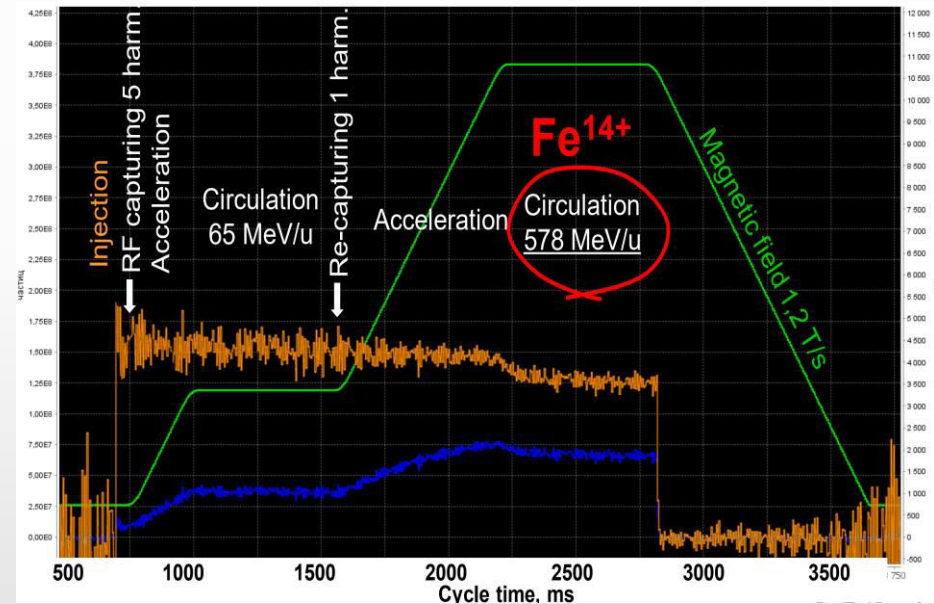


A/q (Target Ion Au^{31+})	6.25
Beam current	< 10 emA
Repetition rate	< 10 Hz
Output energy	3.2 MeV/u

Beam transition through the Booster injection beam line ~ 75%

❖ Stages of the accelerator complex commissioning

- ✓ HILAC + transfer line to Booster → commissioned in 2018 with He^{1+} , Fe^{14+} , C^{4+} , Ar^{14+} and Xe^{28+}
- ✓ HILAC + Booster → first run in November-December, 2020 with He^{1+} , energy up to 100 MeV/u
- ✓ HILAC + Booster + transfer line to Nuclotron → second run in October, 2021 with He^{1+} and Fe^{16+}

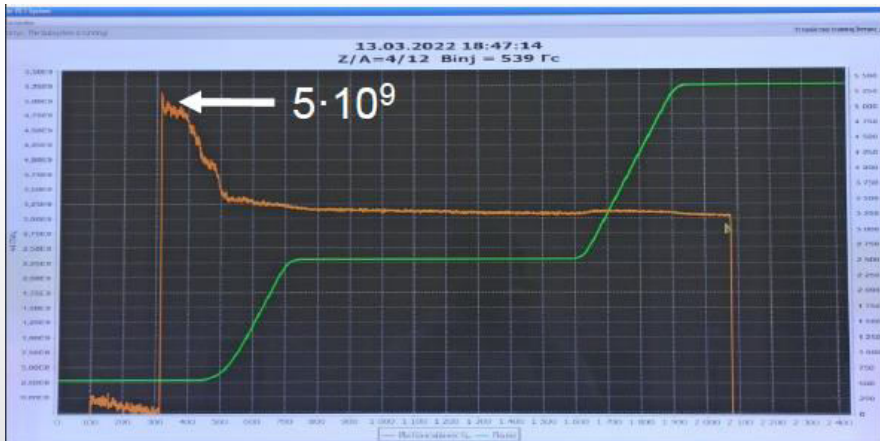


He^+ and Fe^{14+} ions, energy up to 578 MeV/u, residual gas pressure sufficiently low for heavy ions
 Beam extraction from the Booster and transport line to the Nuclotron are put into operation and tuned
 He^+ and Fe^{14+} beams were transported through the beam transfer line to Nuclotron

❖ Stages of the accelerator complex commissioning

- ✓ HILAC + transfer line to Booster → commissioned in 2018 with He^{1+} , Fe^{14+} , C^{4+} , Ar^{14+} and Xe^{28+}
- ✓ HILAC + Booster → first run in November-December, 2020 with He^{1+}
- ✓ HILAC + Booster + transfer line to Nuclotron → second run in October, 2021 with He^{1+} and Fe^{16+}
- ✓ HILAC + Booster + Nuclotron + transfer line to BM@N → third run in Jan.-Apr., 2022 with C^{6+}

Booster



Nuclotron



Average efficiency ~ 30%, non-optimum stripping target thickness

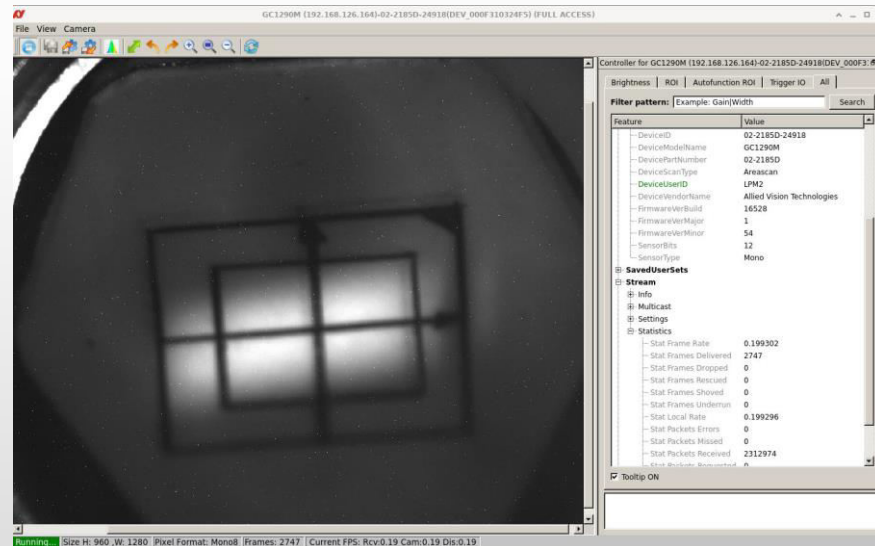
3 GeV/u Carbon beam transported to BM@N area : 5.03 – 29.03

2150 h of the facility operation, BM@N stable operation with beams for 24 days

SRC Collaboration collected 185 M events of carbon interactions with hydrogen target

❖ Stages of the accelerator complex commissioning

- ✓ HILAC + transfer line to Booster → commissioned in 2018 with He^{1+} , Fe^{14+} , C^{4+} , Ar^{14+} and Xe^{28+}
- ✓ HILAC + Booster → first run in November-December, 2020 with He^{1+}
- ✓ HILAC + Booster + transfer line to Nuclotron → second run in October, 2021 with He^{1+} and Fe^{16+}
- ✓ HILAC + Booster + Nuclotron + transfer line to BM@N → third run in Jan. –Apr., 2022 with C^{6+}
- ✓ ESIS + HILAC + Booster + modified Nuclotron + transfer line to BM@N → fourth run started in September, 2022 with Ar and Xe beams



Tuning of Xe acceleration is ongoing, beam of Xe on the phosphor screen at the end section of the Booster-Nuclotron transport line → beams at BM@N to collect $\sim 2 \cdot 10^9$ events

Accelerator, next steps

- ❖ All arc dipole magnets are installed in the tunnel



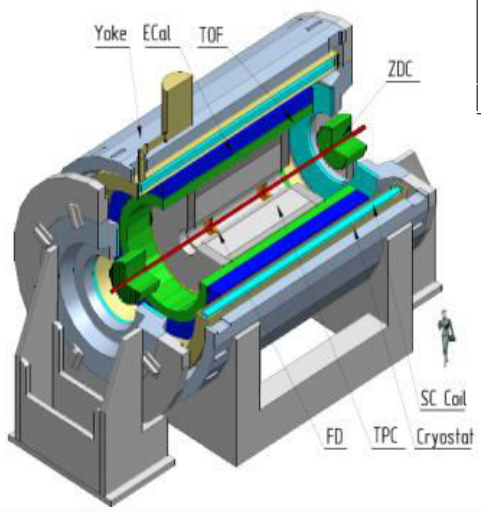
- ❖ Future plans:

- ✓ August-September, 2023 → technological run of NICA without beams
- ✓ End of 2023: first run with beams in the collider rings

See talk by Dr. Anatoly Sidorin on Tuesday for more details

Multi-Purpose Detector

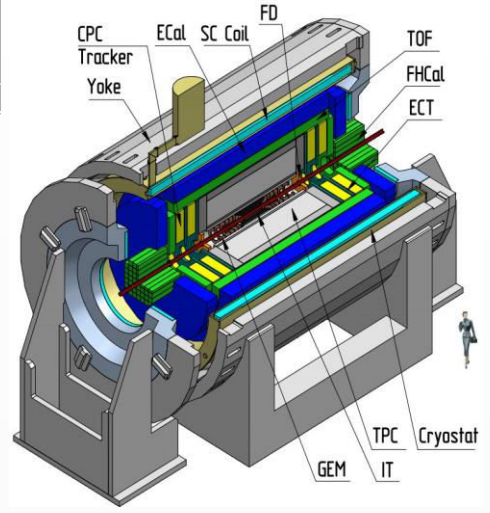
Stage- I



Length	340 cm
Vessel outer radius	140 cm
Vessel inner radius	27 cm
Default magnetic field	0.5 T
Drift gas mixture	90% Ar+10% CH ₄
Maximum event rate	7 kHz ($L = 10^{27} \text{ cm}^{-2} \text{ s}^{-1}$)



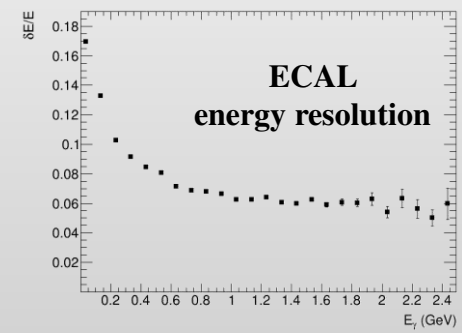
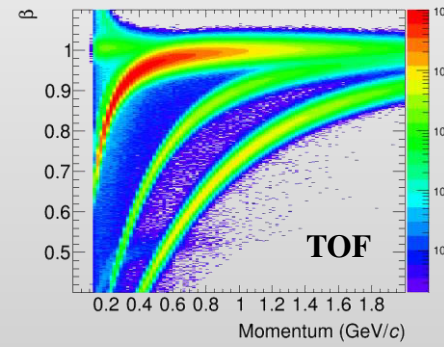
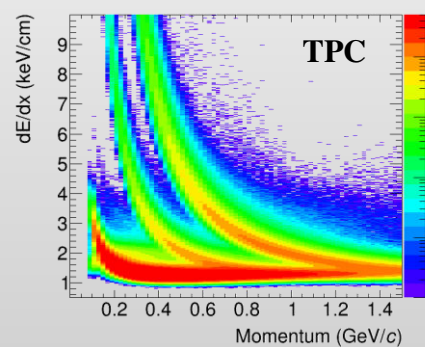
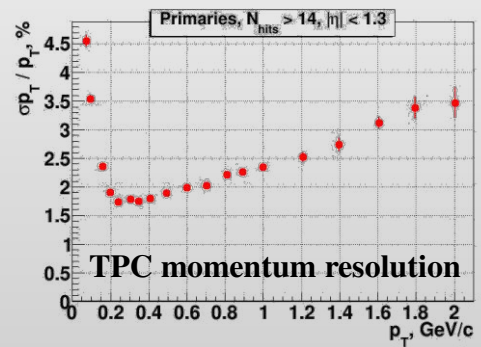
Stage- II



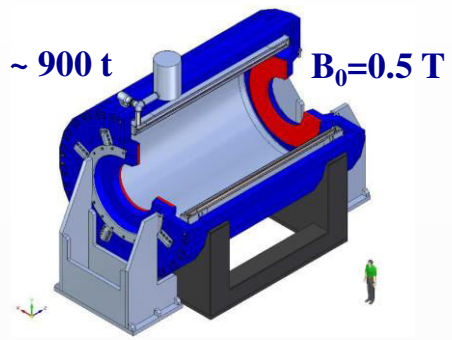
- TPC:** $|\Delta\phi| < 2\pi, |\eta| \leq 1.6$
- TOF, EMC:** $|\Delta\phi| < 2\pi, |\eta| \leq 1.4$
- FFD:** $|\Delta\phi| < 2\pi, 2.9 < |\eta| < 3.3$
- FHCAL:** $|\Delta\phi| < 2\pi, 2 < |\eta| < 5$

- + ITS (heavy-flavor measurements)**
- + forward spectrometers**

Au+Au @ 11 GeV (UrQMD + full chain reconstruction)



SC Solenoid + Iron Yoke



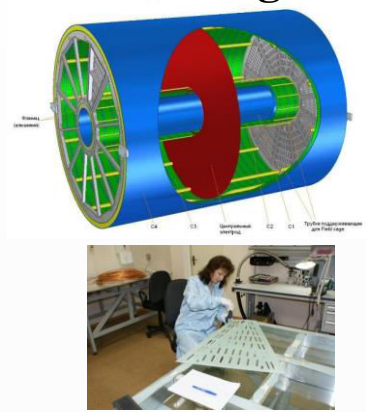
~ 900 t

$B_0=0.5\text{ T}$

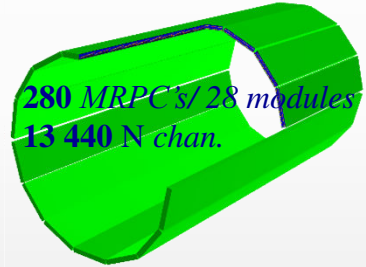
Goal is to cool down and power the magnet + magnetic field measurements in 2023

TPC – central tracking detector

ROCs done
Cylinders done
Electronics in mass production



TOF



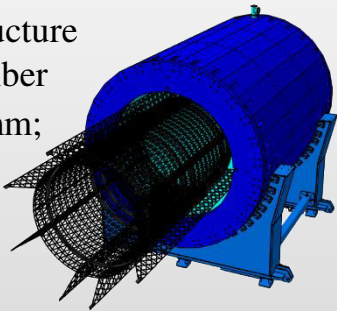
280 MRPCs / 28 modules
13 440 N chan.



~ 100% of MRPCs (modules) are ready, cosmic tests ongoing

Support structure

support structure of carbon fiber
sagite ~ 5 mm;
0,13 X_0

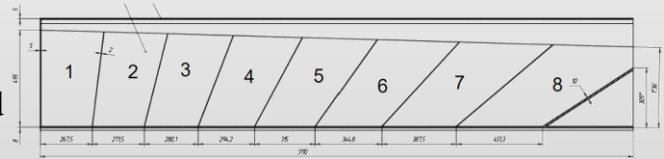


ECAL ~ 100 t

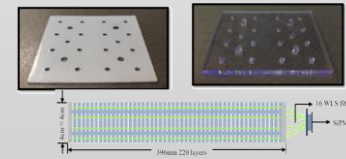
Constructed and delivered

ECAL (projective geometry)

8 sectors = 16 half sectors = 768 modules = 12288 towers



38 400 towers
66-83% of the whole detector will be produced for Stage-I



Pb+Sc "shashlyk"-type towers

See <http://mpd.jinr.ru/doc/mpd-tdr/> for details



- ❖ 2022:
 - ✓ preparation of the SC magnet for cooling
- ❖ 2023:
 - ✓ cooling the magnet and MF measurement
 - ✓ installation of the support frame and detectors
- ❖ 2024:
 - ✓ MPD commissioning
 - ✓ first run with BiBi@9.2 GeV, ~ 50-100 M events for alignment, calibration and physics
- ❖ 2025 and beyond:
 - ✓ Au+Au @ 11 GeV, design luminosity
 - ✓ system size and collision energy scans

- ❖ Preparation of the MPD detector and experimental program is ongoing, all activities are continued
- ❖ All components of the MPD 1-st stage detector are in advanced state of production (subsystems, support frame, electronics platforms, LV/HV, control systems, cryogenics, cabling, etc.)

Schedule of the MPD-NICA is significantly affected by the current geopolitical situation (suspension of collaboration with CERN and Polish & Czech Republic member institutions, economical sanctions and problems with supplies of many components from western companies). The primary goal to have the MPD commissioned by the first beams at NICA collider is preserved.

Multi-Purpose Detector (MPD) Collaboration



MPD International Collaboration was established in 2018 to construct, commission and operate the detector

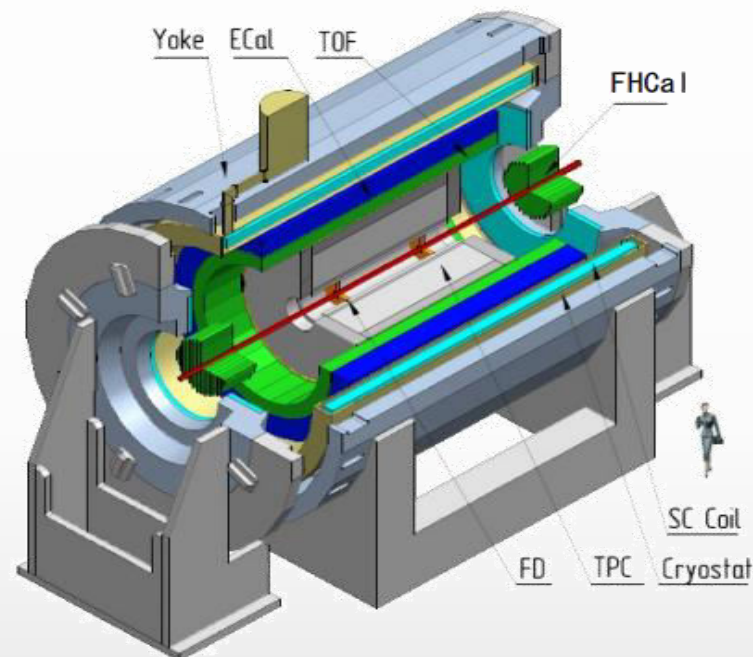
10 Countries, >450 participants, 33 Institutes and JINR

Organization

Acting Spokesperson: **Victor Riabov**
Deputy Spokesperson: **Zebo Tang**
Institutional Board Chair: **Alejandro Ayala**
Project Manager: **Slava Golovatyuk**

Joint Institute for Nuclear Research;

AANL, Yerevan, **Armenia**;
University of Plovdiv, **Bulgaria**;
Tsinghua University, Beijing, **China**;
USTC, Hefei, **China**;
Huzhou University, Huizhou, **China**;
Institute of Nuclear and Applied Physics, CAS, Shanghai, **China**;
Central China Normal University, **China**;
Shandong University, Shandong, **China**;
IHEP, Beijing, **China**;
University of South China, **China**;
Three Gorges University, **China**;
Institute of Modern Physics of CAS, Lanzhou, **China**;
Tbilisi State University, Tbilisi, **Georgia**;
Benemérita Universidad Autónoma de Puebla, **Mexico**;
Centro de Investigación y de Estudios Avanzados, **Mexico**;
Instituto de Ciencias Nucleares, UNAM, **Mexico**;
Universidad Autónoma de Sinaloa, **Mexico**;
Universidad de Colima, **Mexico**;
Universidad de Sonora, **Mexico**;
Institute of Applied Physics, Chisinev, **Moldova**;
Institute of Physics and Technology, **Mongolia**;



Belgorod National Research University, **Russia**;
INR RAS, Moscow, **Russia**;
MEPhI, Moscow, **Russia**;
Moscow Institute of Science and Technology, **Russia**;
North Osetian State University, **Russia**;
NRC Kurchatov Institute, **Russia**;
Plekhanov Russian University of Economics, Moscow, **Russia**;
St. Petersburg State University, **Russia**;
SINP, Moscow, **Russia**;
PNPI, Gatchina, **Russia**;
Vinča Institute of Nuclear Sciences, **Serbia**;
Pavol Jozef Šafárik University, Košice, **Slovakia**



G. Feofilov, A. Aparin

Global observables

- Total event multiplicity
- Total event energy
- Centrality determination
- Total cross-section measurement
- Event plane measurement at all rapidities
- Spectator measurement

V. Kolesnikov, Xianglei Zhu

Spectra of light flavor and hypernuclei

- Light flavor spectra
- Hyperons and hypernuclei
- Total particle yields and yield ratios
- Kinematic and chemical properties of the event
- Mapping QCD Phase Diag.

K. Mikhailov, A. Taranenko

Correlations and Fluctuations

- Collective flow for hadrons
- Vorticity, Λ polarization
- E-by-E fluctuation of multiplicity, momentum and conserved quantities
- Femtoscopy
- Forward-Backward corr.
- Jet-like correlations

V. Riabov, Chi Yang

Electromagnetic probes

- Electromagnetic calorimeter meas.
- Photons in ECAL and central barrel
- Low mass dilepton spectra in-medium modification of resonances and intermediate mass region

Wangmei Zha, A. Zinchenko

Heavy flavor

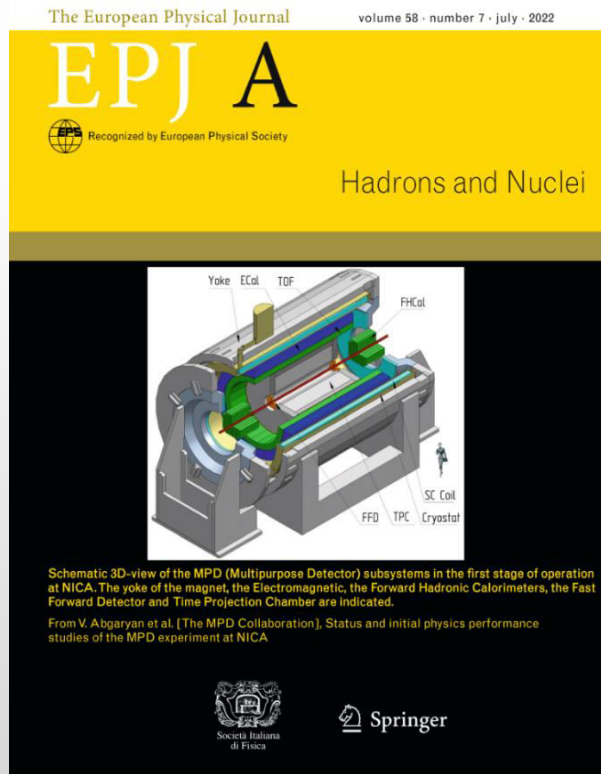
- Study of open charm production
- Charmonium with ECAL and central barrel
- Charmed meson through secondary vertices in ITS and HF electrons
- Explore production at charm threshold

Physics capability studies using centralized Monte Carlo productions:

- ✓ most advanced event generators
- ✓ most up-to-date performance of detector subsystems
- ✓ common detector performance, same event/detector environment for all studies
- ✓ consistent picture for year-1 running with BiBi@9.2 → second collaboration paper

- ❖ Many ongoing construction works, theoretical and physics feasibility studies
- ❖ MPD publications: over 200 in total for hardware, software and physics studies (SPIRES)
- ❖ MPD @ conferences: presented at all major conferences in the field
- ❖ First collaboration paper recently published EPJA (~ 50 pages): Eur.Phys.J.A 58 (2022) 7, 140

Status and initial physics performance studies of the MPD experiment at NICA



Eur. Phys. J. A manuscript No.
(will be inserted by the editor)

Status and initial physics performance studies of the MPD experiment at NICA

The MPD Collaboration¹

¹The full list of Collaboration Members is provided at the end of the manuscript

Received: April 20, 2022 / Accepted: date

1	Abstract	22
2	1	22
3	2	23
4	3	23
5	4	24
6	5	25
7	6	25
8	7	25
9	8	26
10	9	26
11	10	26
12	11	26
13	12	27
14	13	27
15	14	28
16	15	28
17	16	29
18	17	31
19	18	33
20	19	33
21	20	33
22	21	35
23	22	37
24	23	40
25	24	42
26	25	43
27	26	50
28	27	50
29	28	50
30	29	50
31	30	50
32	31	50
33	32	50
34	33	50
35	34	50
36	35	50
37	36	50
38	37	50
39	38	50
40	39	50
41	40	50
42	41	50
43	42	50
44	43	50
45	44	50
46	45	50
47	46	50
48	47	50
49	48	50
50	49	50

1 Introduction

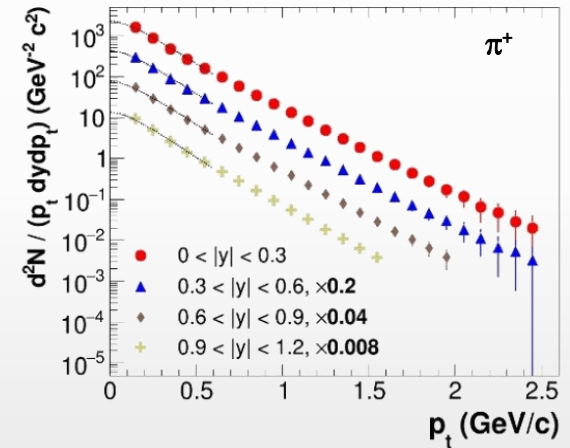
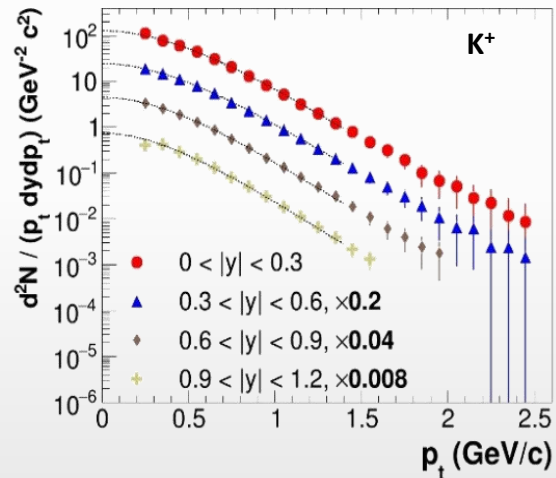
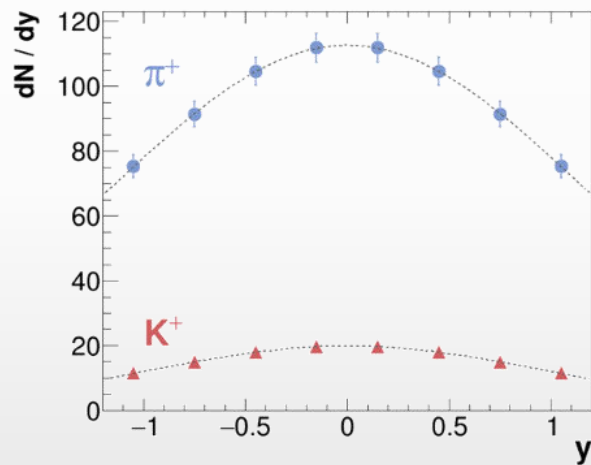
The Multi-Purpose Detector (MPD) is one of the two dedicated heavy-ion collision experiments of the Nuclotron-based Ion Collider Facility (NICA), one of the flagship projects, planned to come into operation at the Joint Institute for Nuclear Research (JINR) in 2022. Its main scientific purpose is to search for novel phenomena in the baryon-rich region of the QCD phase diagram by means of colliding heavy nuclei in the energy range of $4 \text{ GeV} \leq \sqrt{s_{NN}} \leq 11 \text{ GeV}$.

Identified light hadrons

- ❖ Probe freeze-out conditions, collective expansion, hadronization mechanisms, strangeness production (“horn” for K/π), parton energy loss, etc. with particles of different masses, quark contents/counts
- ❖ Charged hadrons: large and uniform acceptance + excellent PID capabilities of TPC and TOF

0-5% central AuAu@9 GeV (PHSD), 5 M events \rightarrow full event/detector simulation and reconstruction

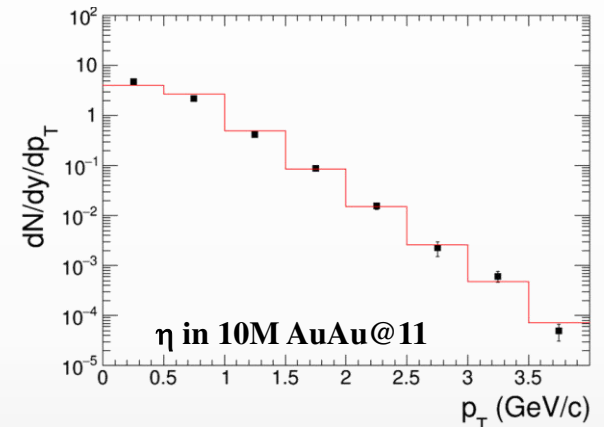
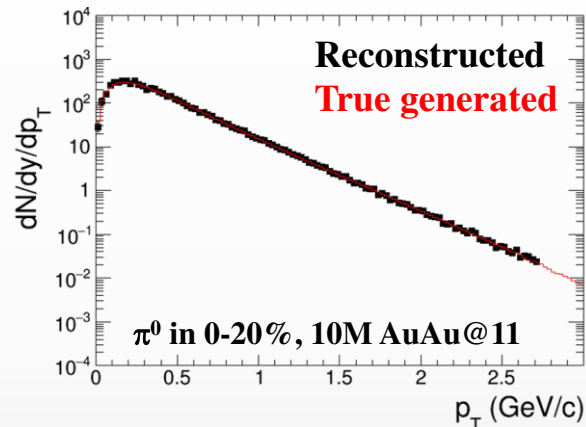
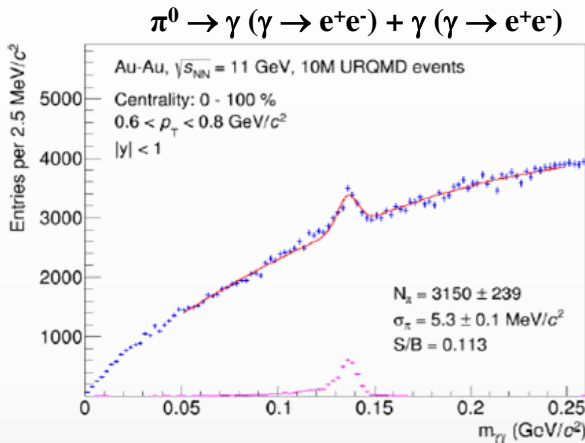
Phys.Part.Nucl. 53 (2022) 2, 203-206



- ✓ sample $\sim 70\%$ of the $\pi/K/p$ production in the full phase space
- ✓ hadron spectra are measured from $p_T \sim 0.1$ GeV/c

- ❖ Neutral mesons (π^0 , η , K_s , ω , η'): ECAL reconstruction + photon conversion method (PCM)

AuAu@11 GeV (UrQMD), 10M events \rightarrow full event/detector simulation and reconstruction



- ✓ extend p_T ranges of charged particle measurements
- ✓ different systematics

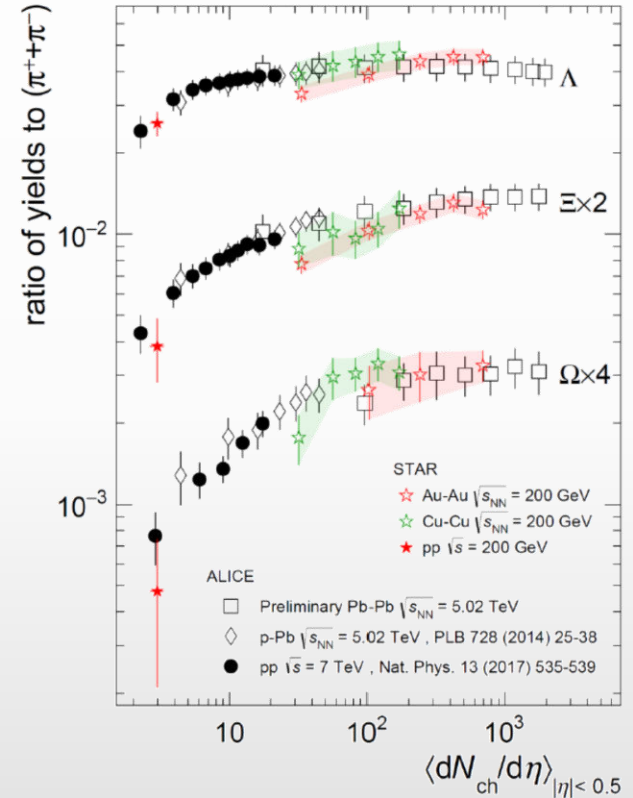
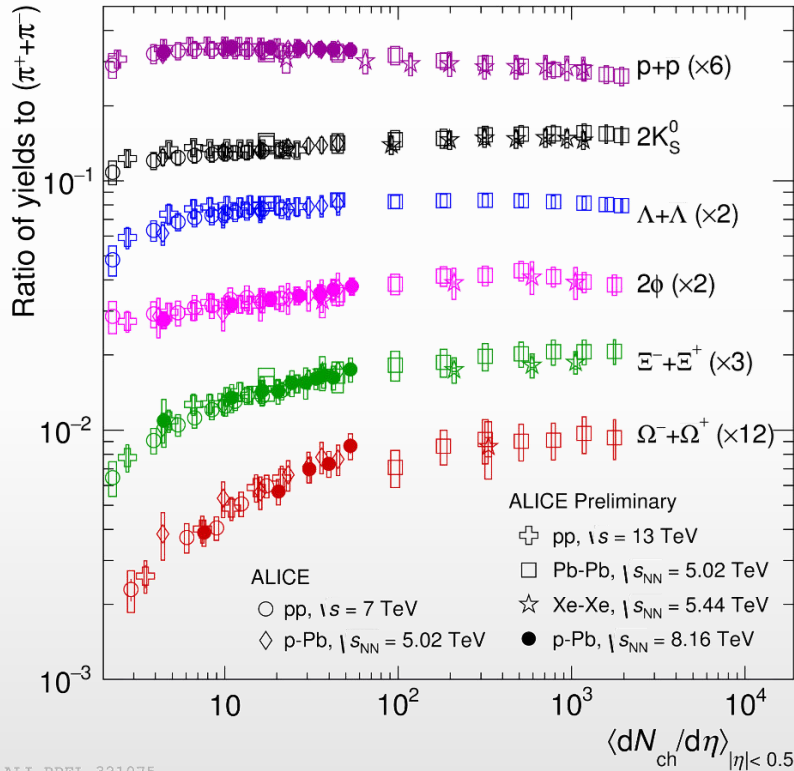
MPD will be able to measure differential production spectra, integrated yields and $\langle p_T \rangle$, particle ratios for a wide variety of identified hadrons (π , K , η , ω , p , η')

First measurements will be possible with a few million sampled heavy-ion events

Strangeness production: pp, p-A, A-A

- ❖ Since the mid 80s, strangeness enhancement is considered as a signature of the QGP formation
- ❖ Experimentally observed in heavy-ion collisions at AGS, SPS, RHIC and LHC energies

Nature Phys. 13 (2017) 535

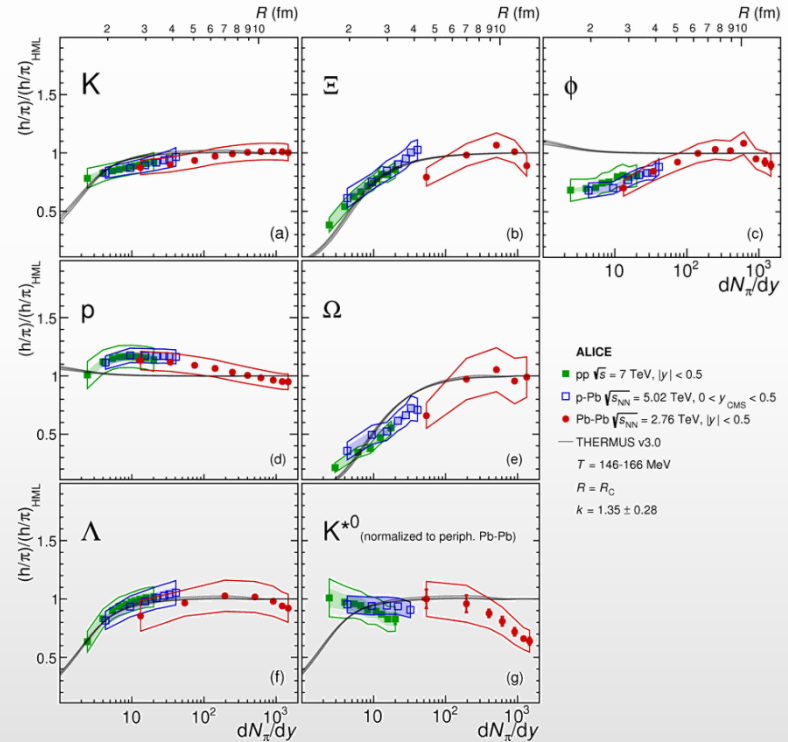
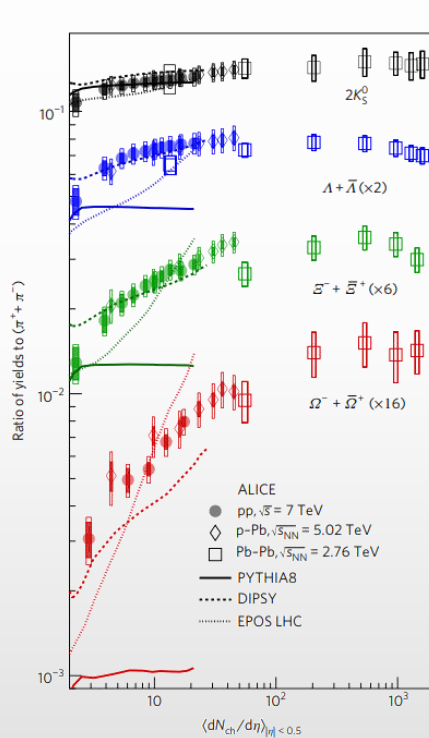


- ❖ Smooth evolution vs. multiplicity in pp, p-A and A-A collisions at LHC energies
- ❖ Strangeness enhancement increases with strangeness content and particle multiplicity
- ❖ STAR @ RHIC measurements in pp, A-A are in agreement with ALICE @ LHC at similar $\langle dN_{ch}/d\eta \rangle$

- ❖ Origin of the strangeness enhancement in small/large systems is still under debate:
 - ✓ strangeness enhancement in QGP contradicts with the observed collision energy dependence
 - ✓ strangeness suppression in pp within canonical suppression models reproduces most of results except for $\phi(1020)$

Nature Physics volume 13, pages535–539 (2017)

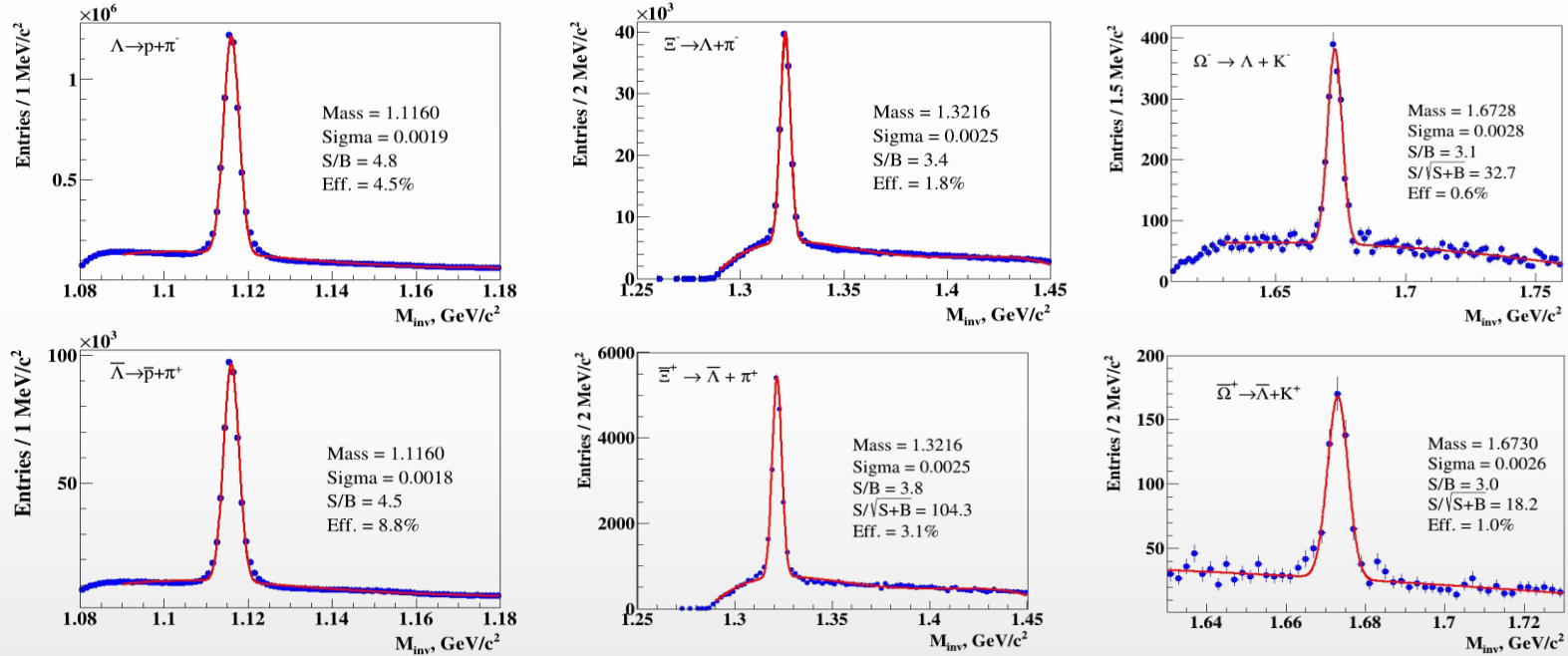
V. Vislavicius, A. Kalweit, arXiv:1610.03001



- ❖ System size scan for (multi)strange baryon and meson production is a key to understanding of strangeness production → unique capability of the MPD in the NICA energy range

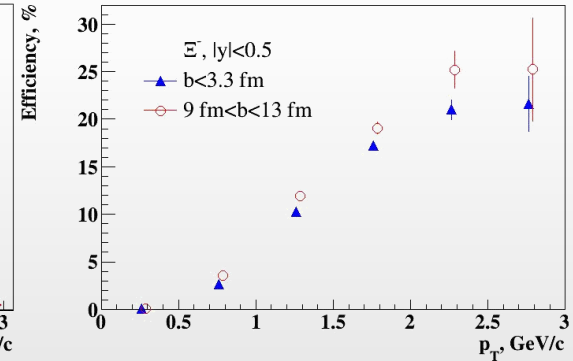
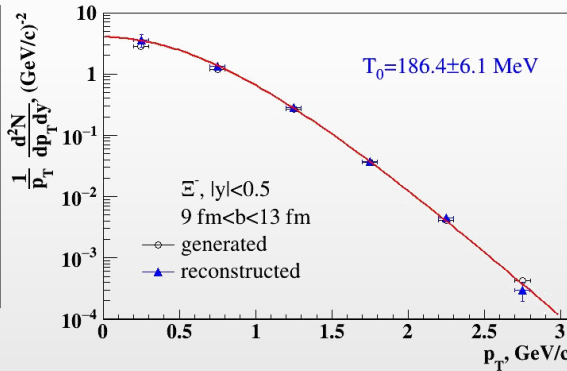
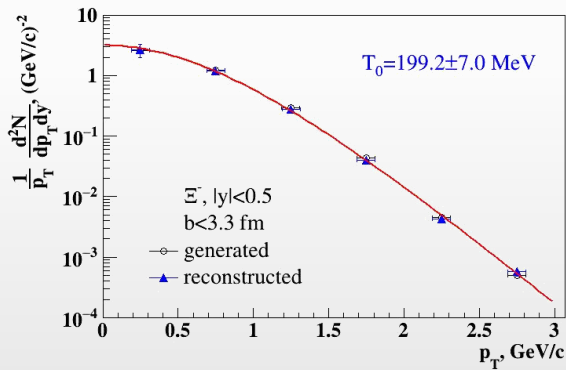
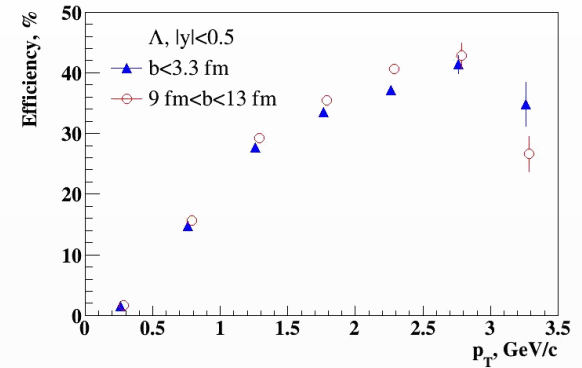
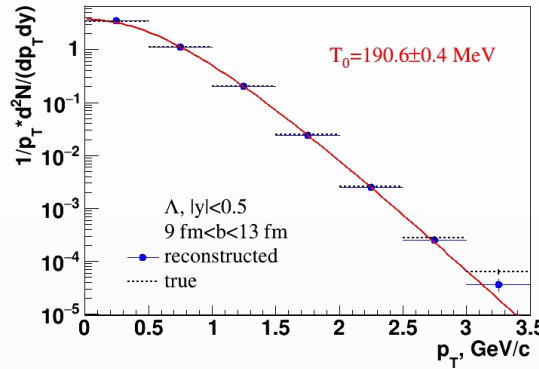
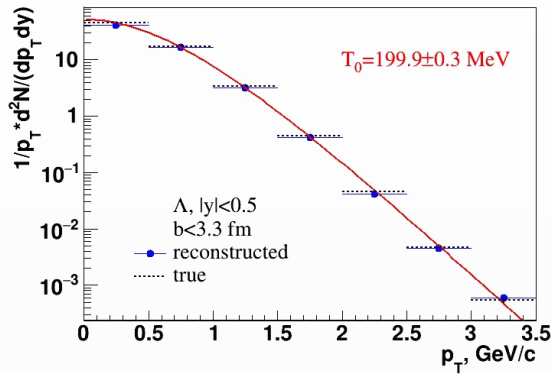
AuAu@11 GeV (PHSD), 10 M events \rightarrow full event/detector simulation and reconstruction

Acta Physica Polonica B 14 (2021) 3, 529-532



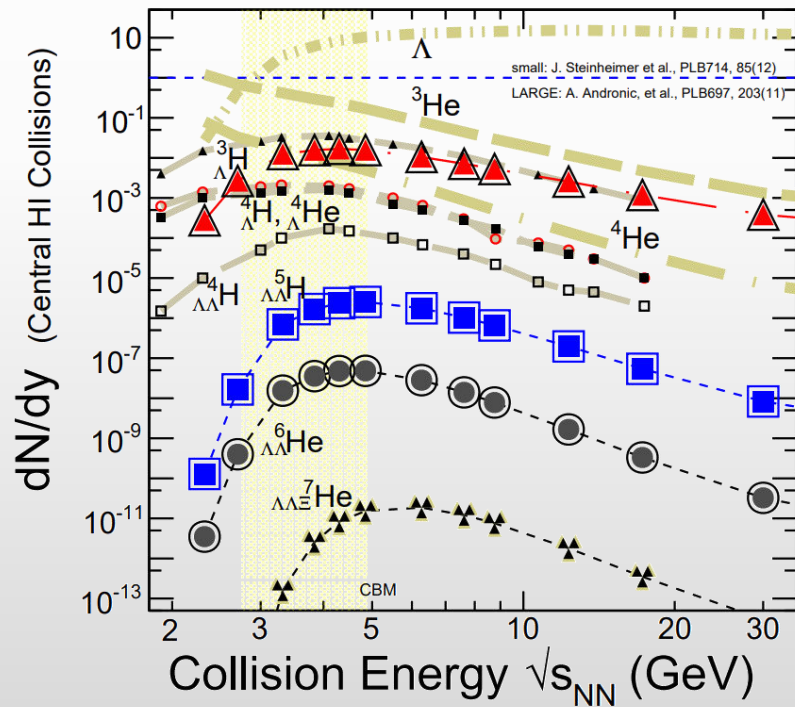
❖ Strange baryons can be reconstructed with good S/B ratios using charged hadron identification in the TPC&TOF and different decay topology selections

❖ Reconstructed spectra are consistent with the generated ones

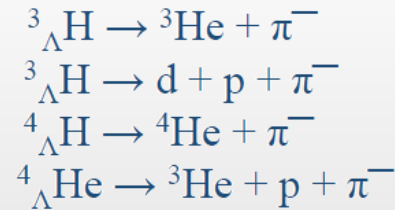


MPD has capabilities to measure production of charged $\pi/K/p$ and (multi)strange baryons in pp, p-A and A-A collisions using charged hadron identification in TPC&TOF and different decay topology selections

- ❖ Hyper nuclei measurement studies are crucial:
 - ✓ microscopic production mechanism, Y-N potential, strange sector of nuclear EoS
 - ✓ strong implications for astrophysics → hyperons expected to exist in the inner core of neutron stars
- ❖ Production mechanism usually described with two classes of phenomenological models :
 - ✓ statistical hadronization (SHM) → production during phase transition, $dN/dy \propto \exp(-m/T_{\text{chem}})$ [1]
 - ✓ coalescence → (anti)nucleons close in phase space ($\Delta p < p_0$) and matching the spin state form a nucleus [2]
- ❖ Models predict enhanced hypernuclear production at NICA → double hypernuclei are reachable



- ❖ Reconstruction of hypernuclei requires detection and identification of light nuclei and precise secondary vertex reconstruction:

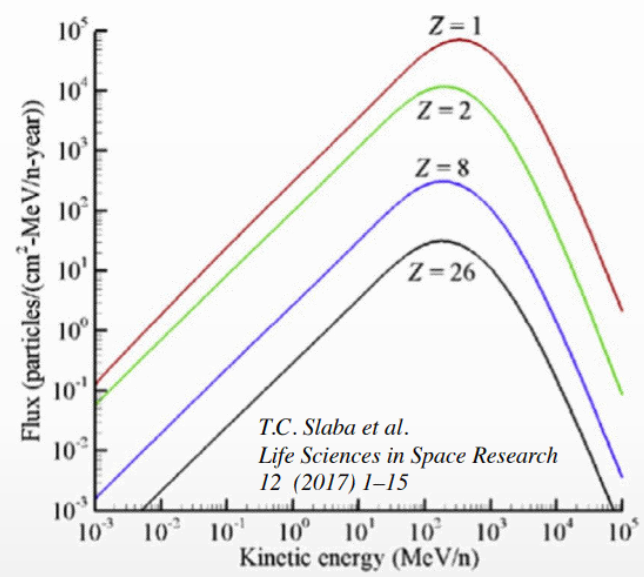


- ❖ Observables of interest: precise measurements of binding energies, lifetimes and branching ratios

[1] Andronic et al., Nature 561 (2018) 321–330

[2] Butler et al., Phys. Rev. 129 (1963) 836

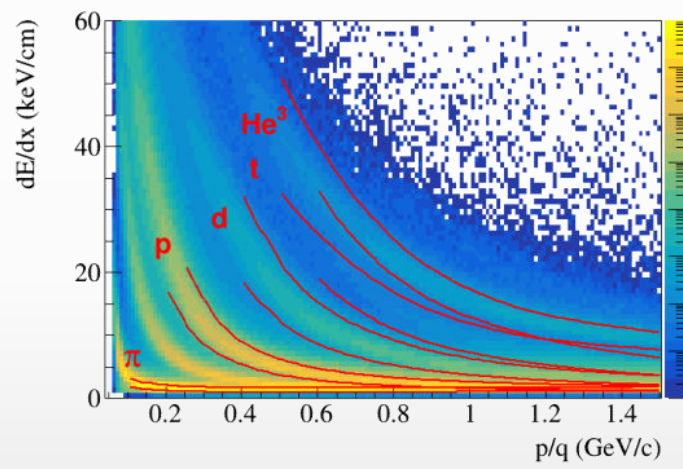
- ❖ Galactic Cosmic Rays composed of nuclei (protons, ... up to Fe) and E/A up to 50 GeV
- ❖ These high-energy particles create cascades of hundreds of secondary, etc. particles



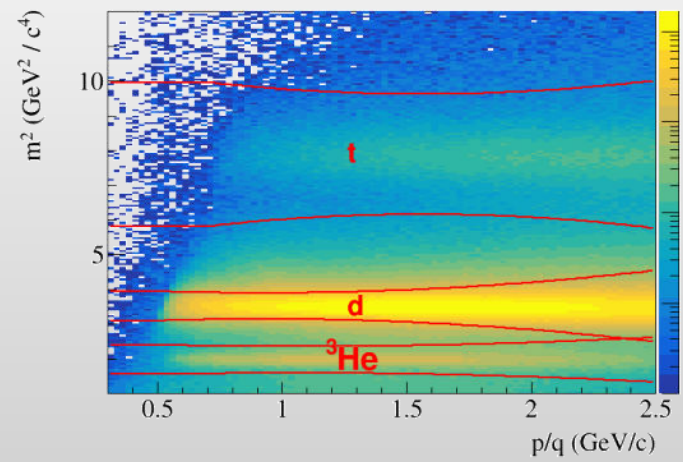
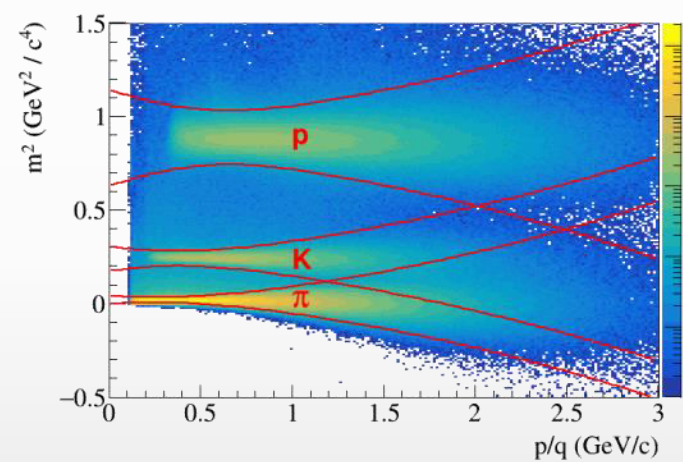
- ❖ Cosmic rays are a serious concern to astronauts, electronics, and spacecraft.
- ❖ The damage is proportional to Z^2 , contribution of secondaries p, d, t, ^3He , and ^4He is also significant
- ❖ Need input information for transport codes for shielding applications (Geant-4, Fluka, PHITS, etc.):
 - ✓ total, elastic/reaction cross section
 - ✓ particle multiplicities and coellocense parameters
 - ✓ outgoing particle distributions: $d^2N/dEd\Omega$

- ❖ NICA can deliver different ion beam species and energies:
 - ✓ Targets of interest (C = astronaut, Si = electronics, Al = spacecraft) + He, C, O, Si, Fe, etc.
- ❖ No data exist for projectile energies > 3 GeV/n

dE/dx vs momentum in TPC



m² vs. momentum in TOF

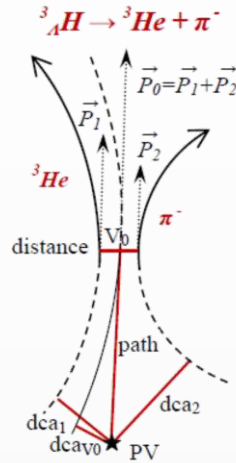
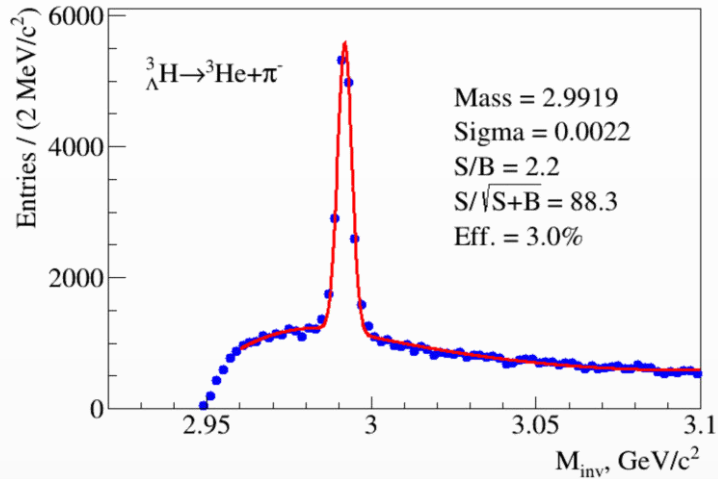


MPD has excellent light fragment identification capabilities in a wide rapidity range → unique capability of the MPD in the NICA energy range

Reconstruction of hypertritons

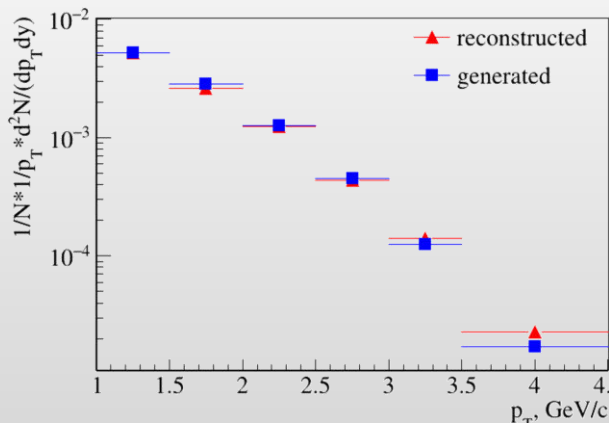
BiBi@9.2 GeV (PHQMD), 40 M events → full event/detector simulation and reconstruction

Phys.Part.Nucl.Lett. 19 (2022) 1, 46-53

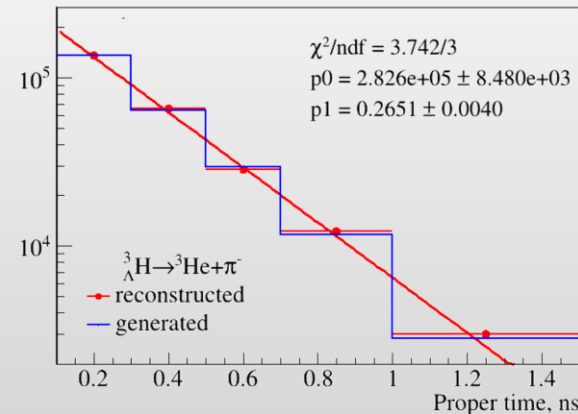


Decay channel	Branching ratio	Decay channel	Branching ratio
$\pi^- + {}^3\text{He}$	24.7%	$\pi^- + p + p + n$	1.5%
$\pi^0 + {}^3\text{H}$	12.4%	$\pi^0 + n + n + p$	0.8%
$\pi^- + p + d$	36.7%	$d + n$	0.2%
$\pi^0 + n + d$	18.4%	$p + n + n$	1.5%

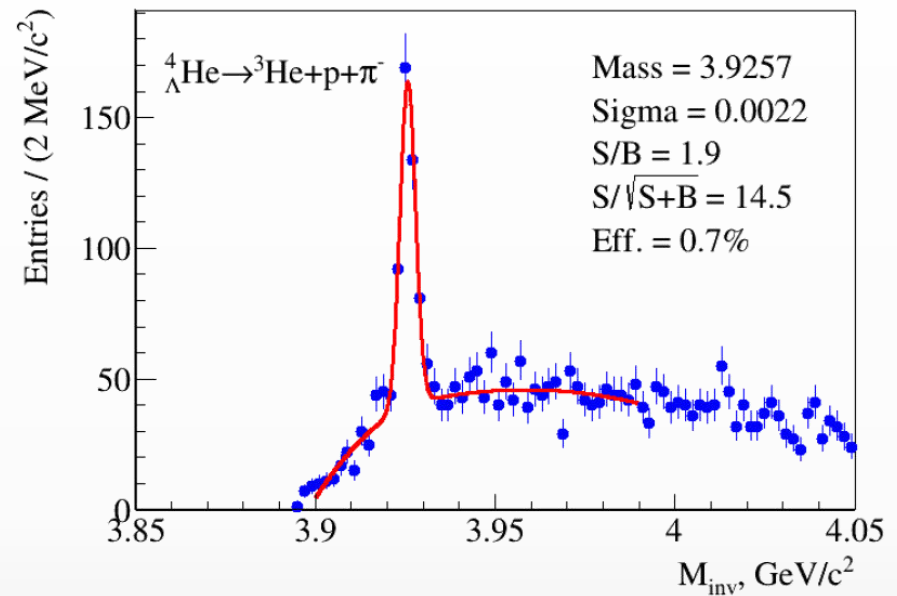
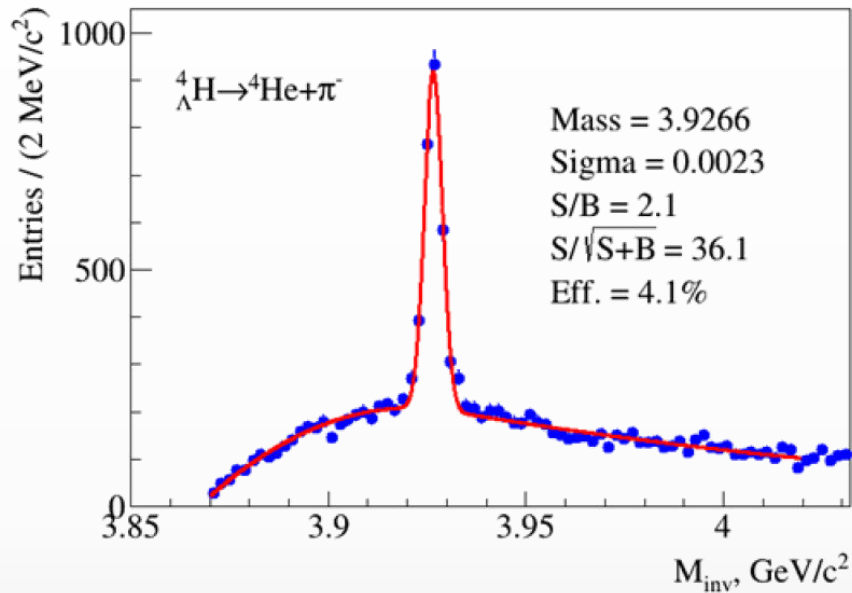
Spectrum is reconstructed up to $p_T=4.5$ GeV/c



$$N(\tau) = N(0) \exp\left(-\frac{\tau}{\tau_0}\right) = N(0) \exp\left(-\frac{ML}{cp\tau_0}\right),$$



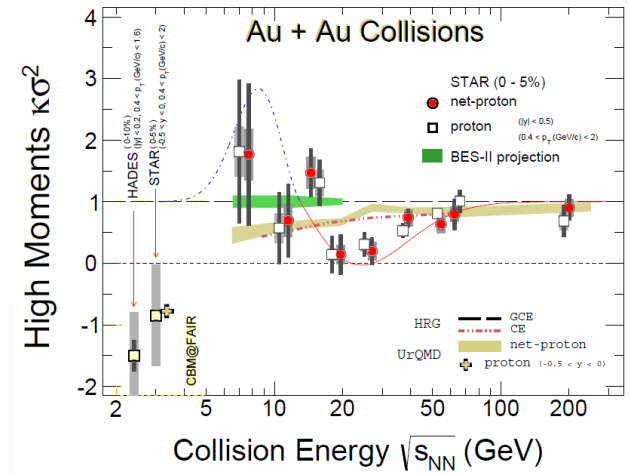
❖ First measurements for hypertriton will be possible with accumulation of ~ 50 M BiBi@9.2 events



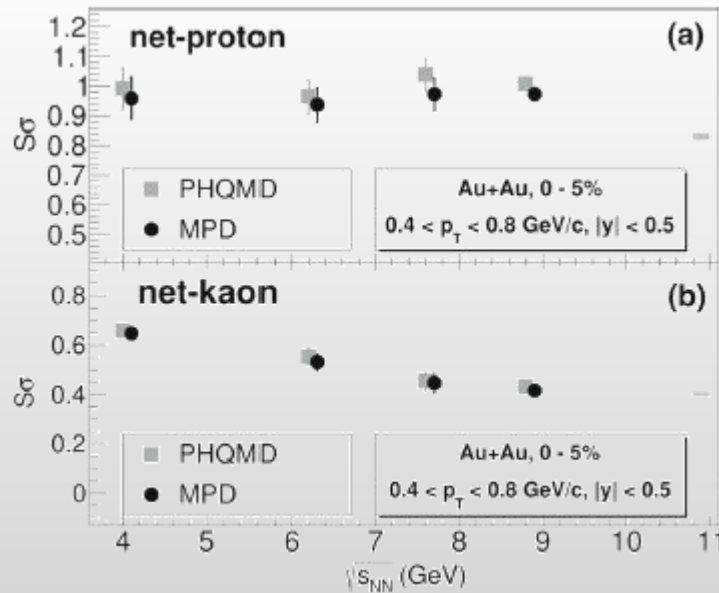
- ❖ Monte Carlo events enriched with hypernuclei distributed by $(\eta-p_T)$ phase space predicted by PHQMD
- ❖ Signals for heavier hypernuclei can be reconstructed with the equivalent statistics of ~ 140 M events

Critical fluctuations

- ❖ Ratio of the 4th-to2nd moments of the (net)proton multiplicity:
 - ✓ non-monotonic behavior → deviation from non-critical dynamic baseline close to CEP ???
 - ✓ need significant improvement of statistical precision and systematic uncertainties + extra points in the NICA energy range



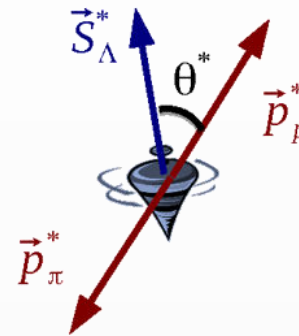
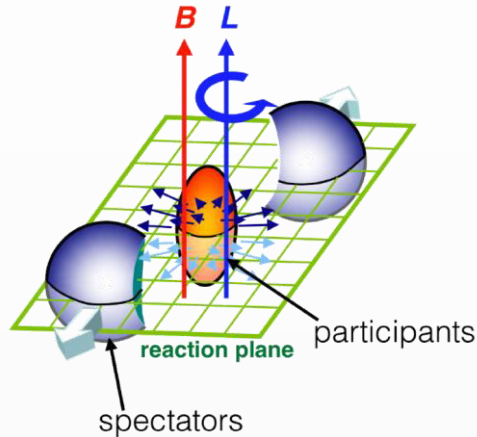
AuAu@11 (UrQMD), $5 \cdot 50 \cdot 10^4$ events → full event/detector simulation and reconstruction



Effective skewness $S\sigma$ for net-protons (a) and net-kaons (b) in Au+Au interactions at several collision energies are reproduced

Global hyperon polarization

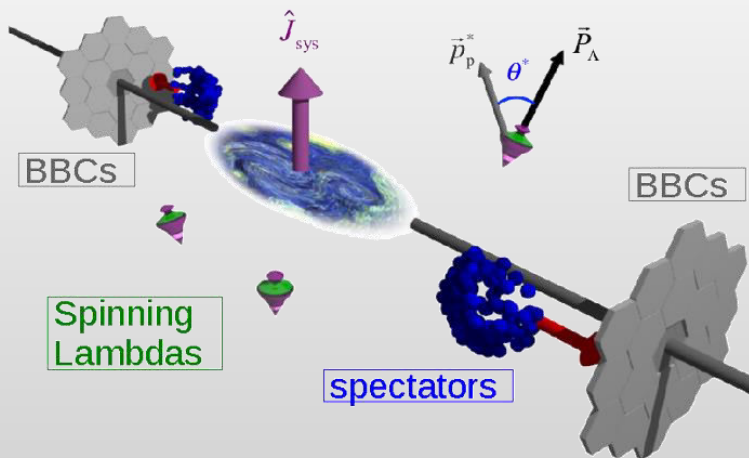
- ❖ Large angular momentum and strong magnetic field formed in mid-central heavy-ion collisions → polarization of particles in the final state



- ❖ $\Lambda/\bar{\Lambda}$ are “self-analyzing” probes → preferential emission of proton in in spin direction

STAR, Nature 548, 62 (2017)

Phys.Rev.Lett.94:102301,2005;
Erratum-ibid.Lett.96:039901,2006



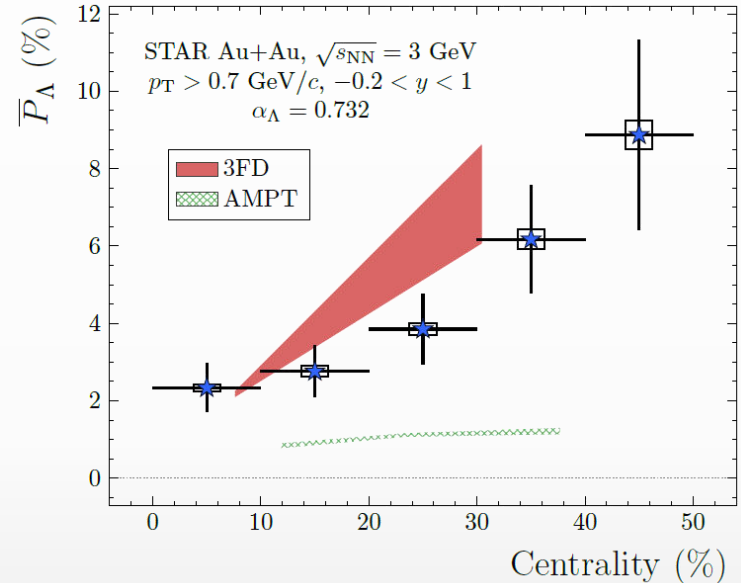
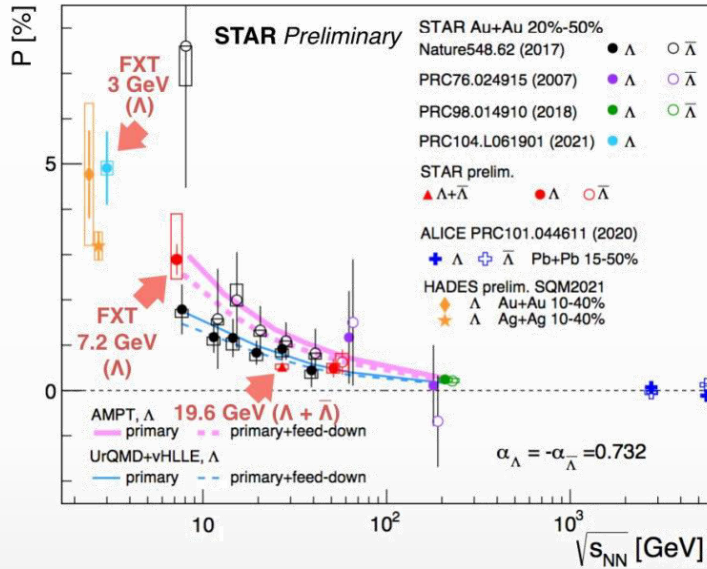
The global polarization observable is defined by [34](#):

$$P_{\Lambda} = \frac{8}{\pi\alpha_{\Lambda}} \frac{\langle \sin(\Psi_{EP} - \phi_p^*) \rangle}{R_{EP}}. \quad (1)$$

Here $\alpha_{\Lambda} = 0.732 \pm 0.014$ [35](#) is the Λ decay parameter, Ψ_{EP} the event plane angle, ϕ_p^* the azimuthal angle of the proton in the Λ rest frame, R_{EP} the resolution of the event plane angle and the brackets $\langle \cdot \rangle$ denote the average

- ❖ Global hyperon polarization measurements in mid-central A+A collisions at $\sqrt{s_{NN}} = 3-5000$ GeV

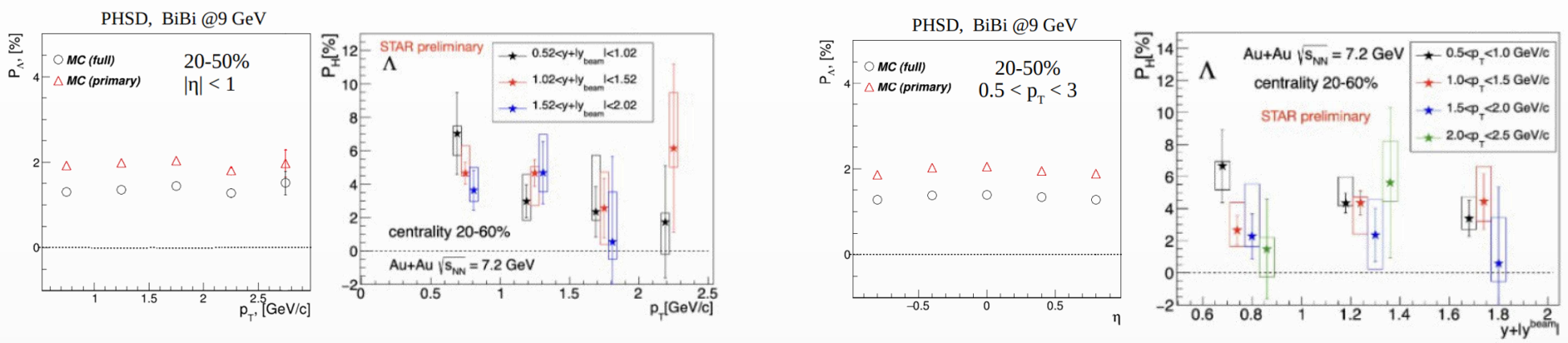
STAR, Phys.Rev.C, 104(6):L061901, 2021



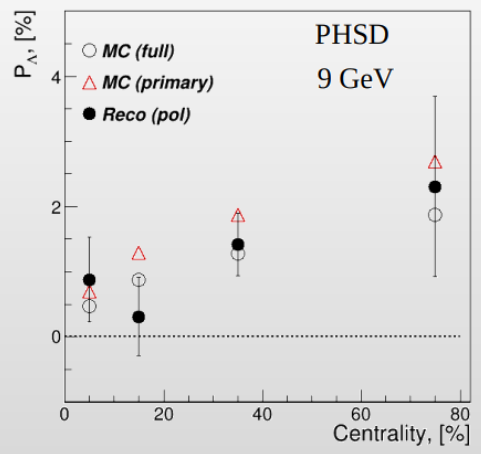
- ❖ Global polarization of hyperons experimentally observed, decreases with $\sqrt{s_{NN}}$
- ❖ Hint for a $\Lambda - \bar{\Lambda}$ difference, magnetic field, $P_\Lambda \simeq \frac{1}{2} \frac{\omega}{T} + \frac{\mu_\Lambda B}{T}$, $P_{\bar{\Lambda}} \simeq \frac{1}{2} \frac{\omega}{T} - \frac{\mu_\Lambda B}{T}$?
- ❖ Feed down from $\Sigma(1385) \rightarrow \Lambda\pi$, $\Sigma^0 \rightarrow \Lambda\gamma$; $\Xi \rightarrow \Lambda\pi$ reduces polarization by $\sim 10-20\%$
- ❖ Energy dependence of global polarization is reproduced by AMPT, 3FD, UrQMD+vHLLLE
- ❖ AMPT with partonic transport strongly underestimates measurements at $\sqrt{s_{NN}} = 3$ GeV \rightarrow hadron gas?

MPD: extra points in the energy range 3-10 10 GeV with small uncertainties; centrality, p_T and rapidity dependence of polarization not only for Λ , but other (anti)hyperons (Λ , Σ , Ξ)

- ❖ BiBi@9.2 GeV (PHSD), ~1 M events → full event/detector simulation and reconstruction
- ❖ Global hyperon polarization (thermodynamical Becattini approach [1]) by the event generator → reproduce at generator level basic features measured by STAR

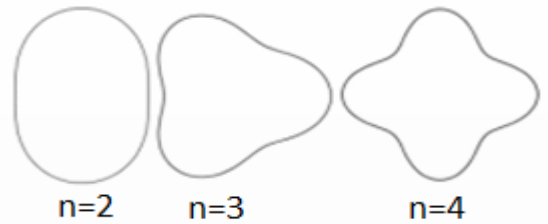
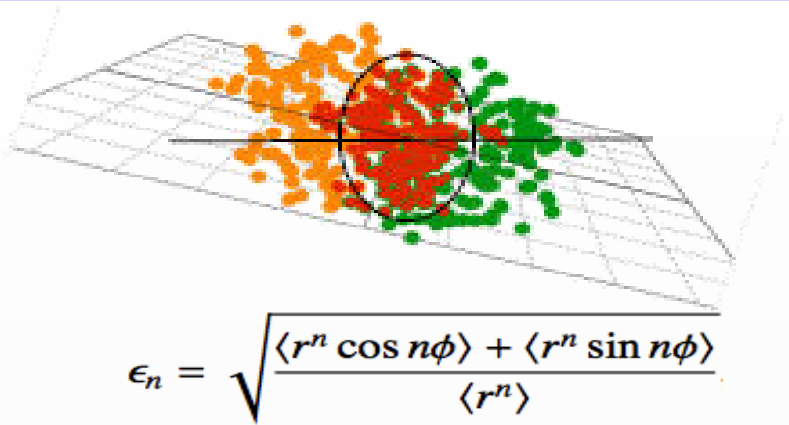


- ❖ Reconstruction of Λ global polarization with 1M sampled AuAu@9 events (work in progress):



- ❖ Measured polarization is consistent with the generated one
- ❖ First global polarization measurements for $\Lambda/\bar{\Lambda}$ will be possible with ~ 10M data sampled events

[1] F. Becattini, V. Chandra, L. Del Zanna, E. Grossi, Ann. Phys. 338 (2013) 32

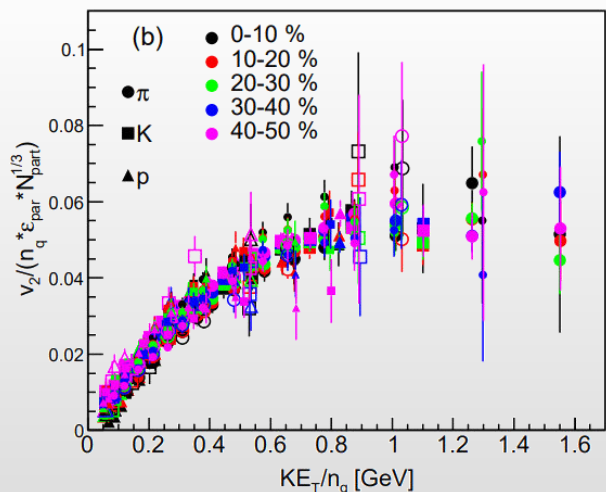
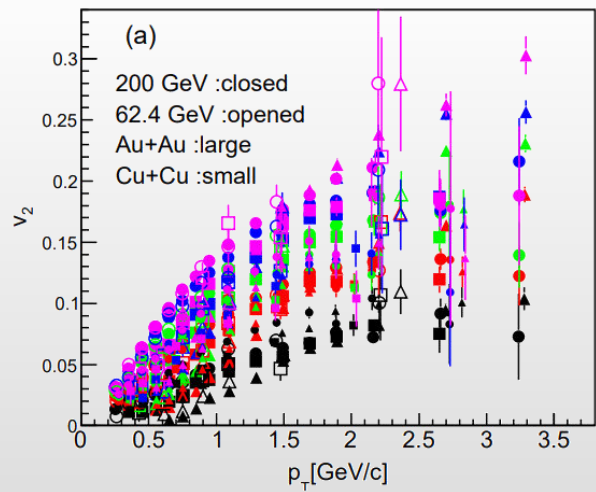
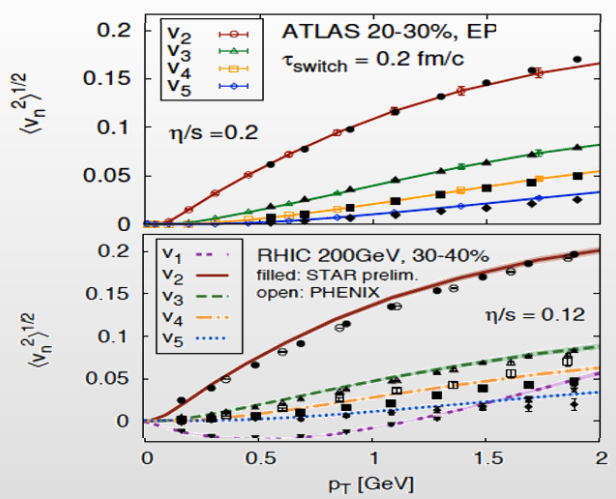


$$\frac{dN}{d\phi} \propto \left(1 + 2 \sum_{n=1} v_n \cos [n(\phi - \Psi_n)] \right)$$

❖ Initial eccentricity and its fluctuations drive momentum anisotropy v_n with specific viscous modulation

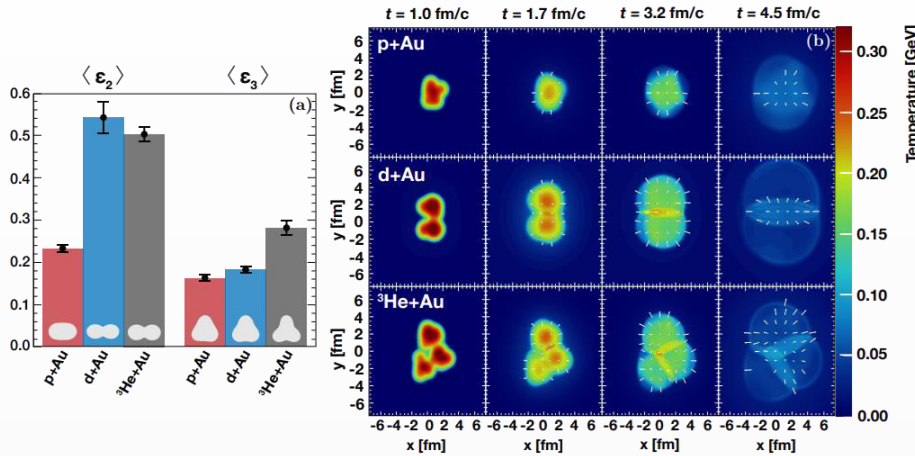
Gale, Jeon et al., Phys. Rev. Lett. 110, 012302

Phys.Rev.C 92 (2015) 3, 034913



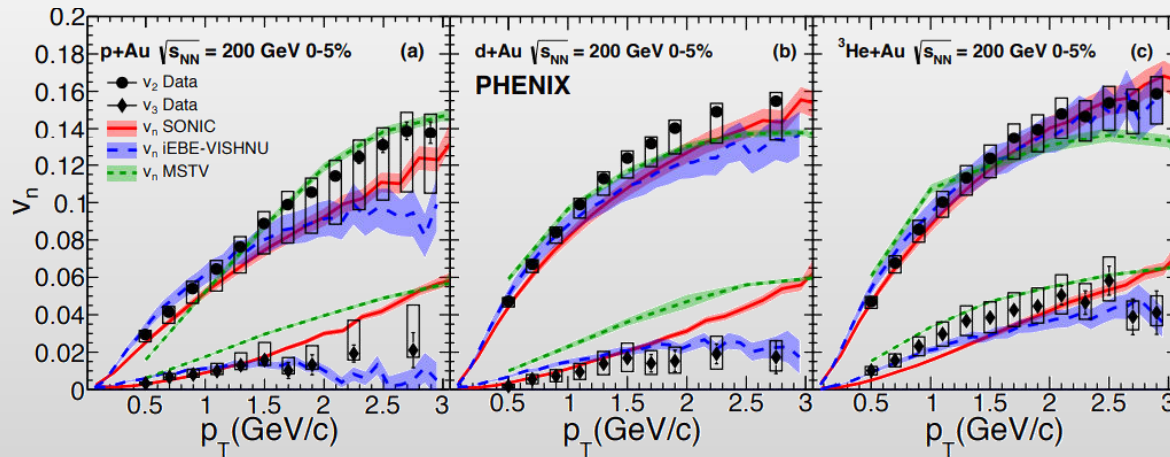
❖ Evidence for a dense perfect liquid found at RHIC/LHC (M. Roizard et al., Scientific American, 2006)

❖ System size scan (A-A) is an important part of systematic study (initial geometry \rightarrow flow harmonics)

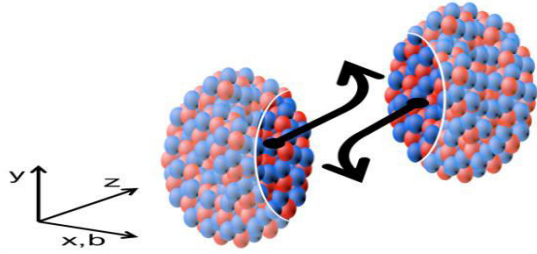


p-Au, d-Au and ^3He -Au @ 200 GeV by PHENIX

- ❖ Measurements demonstrate that the v_n 's are correlated to the initial geometry
- ❖ Hydrodynamical models, which include the formation of a short-lived QGP droplet, provide a simultaneous description of these measurements

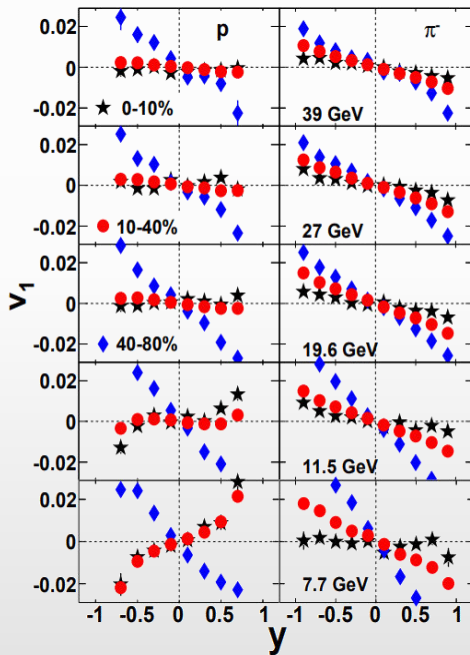


Beam energy dependence



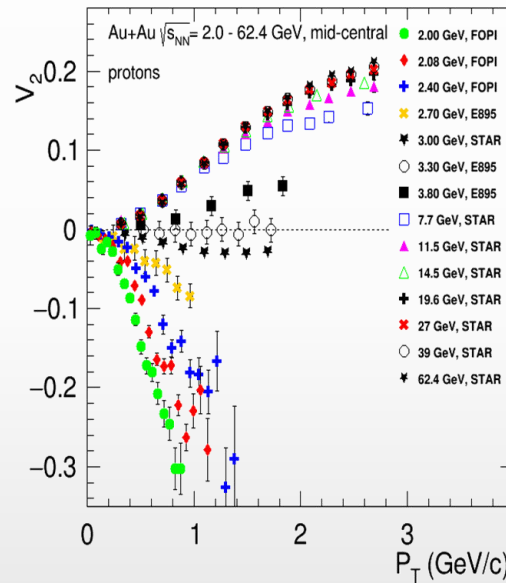
- ❖ Generated during the nuclear passage time $(2R/\gamma)$ – sensitive to EOS
- ❖ RHIC @ 200 GeV $(2R/\gamma) \sim 0.1$ fm/c
- ❖ AGS @ 3-4.5 GeV $(2R/\gamma) \sim 9-5$ fm/c
- ❖ v_1 and v_2 show strong centrality, energy and species dependence

Phys.Rev.Lett. 112 (2014) 16, 162301

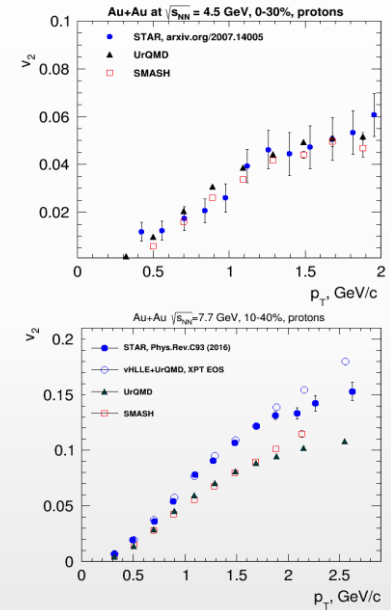


models do not reproduce measurements

EPJ Web Conf. 204 (2019) 03009

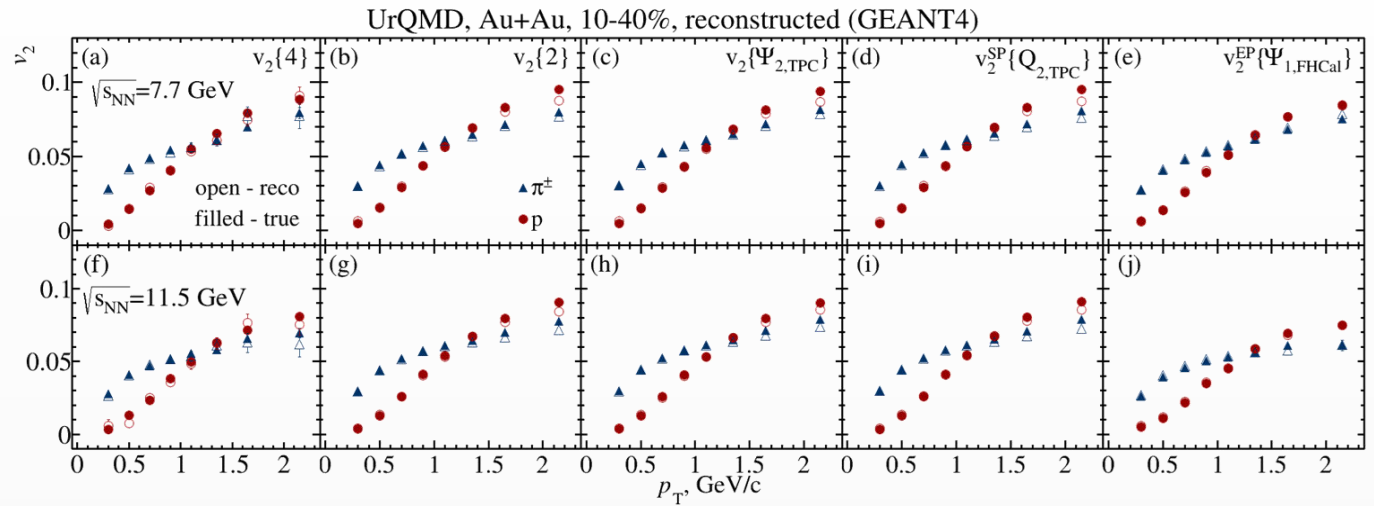


- ✓ $\sqrt{s_{NN}} \sim 3-4.5$ GeV, pure hadronic models reproduce v_2 (JAM, UrQMD) \rightarrow degrees of freedom are the interacting baryons
- ✓ $\sqrt{s_{NN}} \geq 7.7$ GeV, need hybrid models with QGP phase (vHLLE+UrQMD, AMPT with string melting,...)

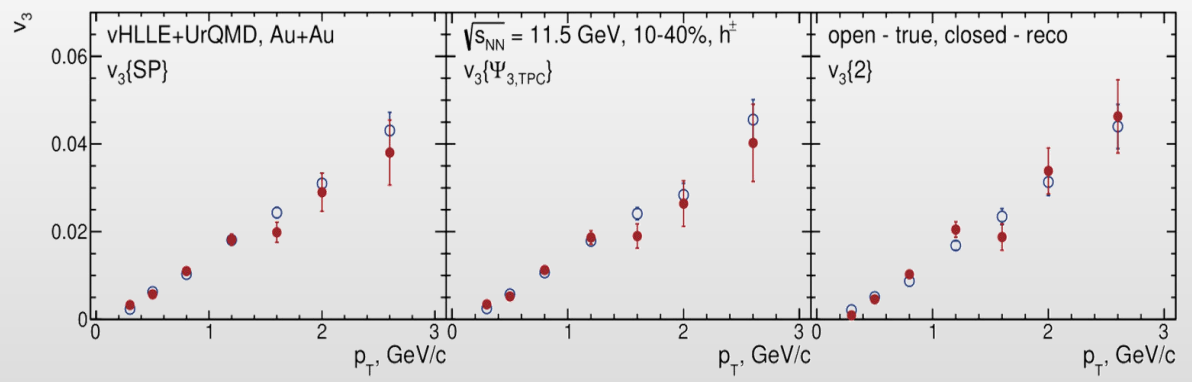


System size scan for flow measurements is vital for understanding of the medium transport properties and onset of the phase transition \rightarrow unique capability of the MPD in the NICA energy range

AuAu@7.7 GeV (UrQMD), 15 M events \rightarrow full event/detector simulation and reconstruction



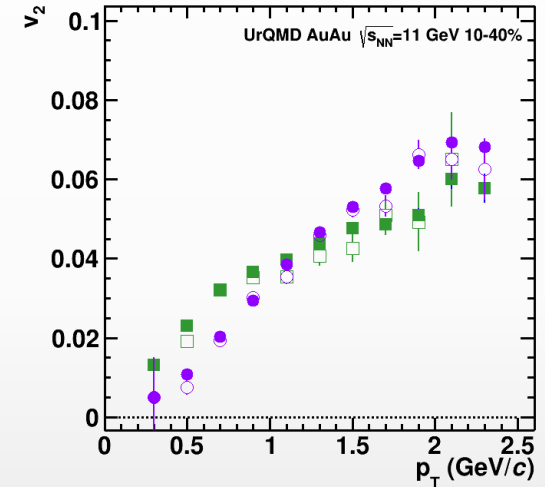
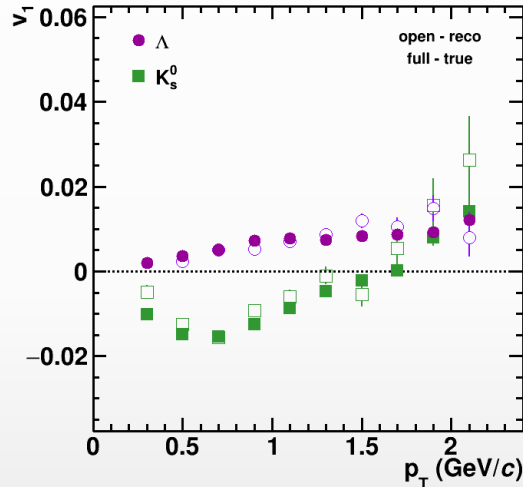
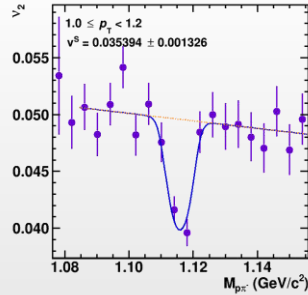
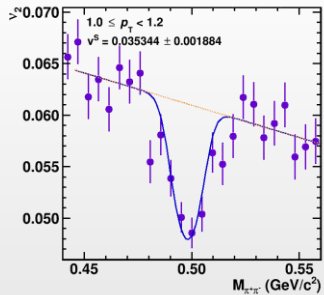
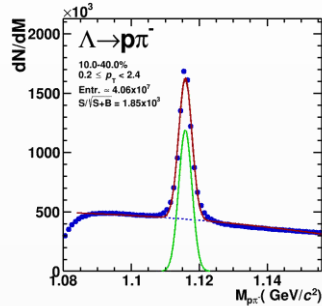
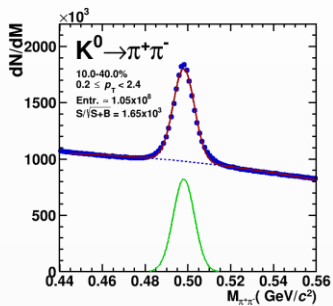
AuAu@11.5 GeV (vHLLE + UrQMD), 15 M events \rightarrow full event/detector simulation and reconstruction



- ❖ Reconstructed and generated v_2 of pions and protons and v_3 of charged hadrons are in good agreement
- ❖ Models show that higher harmonic ripples are more sensitive to the existence of a QGP phase

AuAu@11 GeV (UrQMD), 25 M events \rightarrow full event/detector simulation and reconstruction

$$v_2^{SB}(\mathbf{m}_{inv}, \mathbf{p}_T) = v_2^S(\mathbf{p}_T) \frac{N^S(\mathbf{m}_{inv}, \mathbf{p}_T)}{N^{SB}(\mathbf{m}_{inv}, \mathbf{p}_T)} + v_2^B(\mathbf{m}_{inv}, \mathbf{p}_T) \frac{N^B(\mathbf{m}_{inv}, \mathbf{p}_T)}{N^{SB}(\mathbf{m}_{inv}, \mathbf{p}_T)}$$



- ❖ Differential flow signal extraction using invariant mass fit method
- ❖ Reasonable agreement between reconstructed and generated v_n signals for K_S^0 and Λ

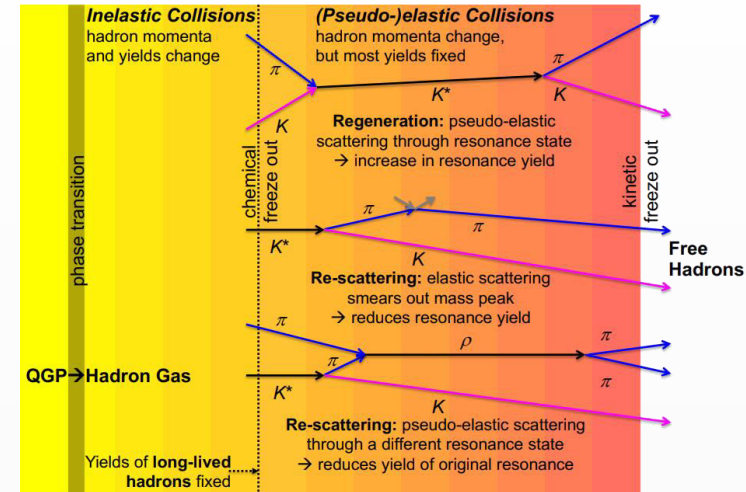
- ❖ Resonances are best suited to probe density and lifetime of the late hadronic phase of HI collisions

increasing lifetime \longrightarrow

	$\rho(770)$	$K^*(892)$	$\Sigma(1385)$	$\Lambda(1520)$	$\Xi(1530)$	$\phi(1020)$
$c\tau$ (fm/c)	1.3	4.2	5.5	12.7	21.7	46.2
σ_{rescatt}	$\sigma_{\pi}\sigma_{\pi}$	$\sigma_{\pi}\sigma_K$	$\sigma_{\pi}\sigma_{\Lambda}$	$\sigma_K\sigma_p$	$\sigma_{\pi}\sigma_{\Xi}$	$\sigma_K\sigma_K$

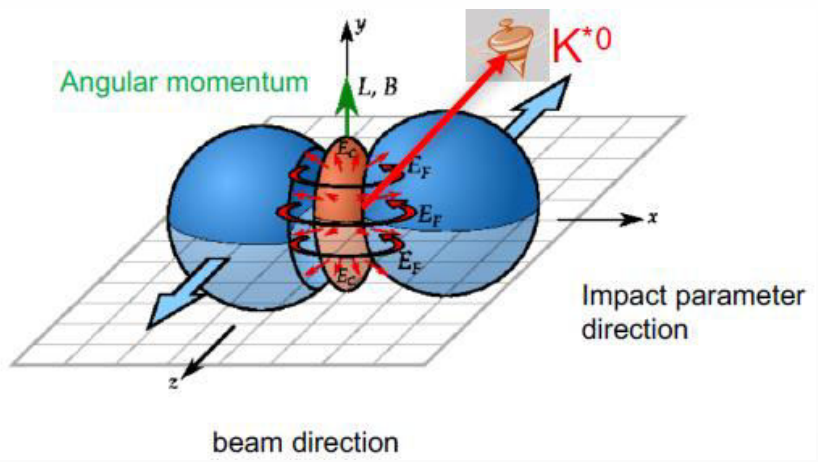
Final state yields of resonances depend on:

- resonance yields at chemical freeze-out
- lifetime of the resonance and the hadronic phase
- type and scattering cross sections of daughter particles



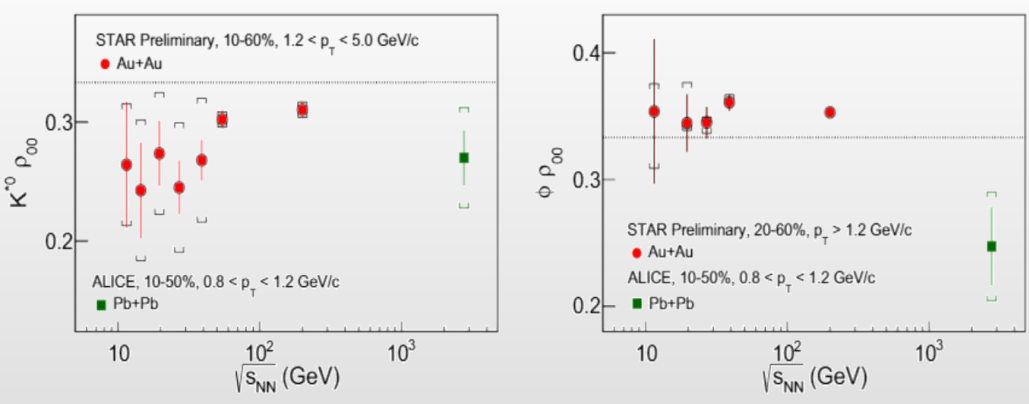
- ❖ Suppression of short-lived ρ^0 , $K^*(892)^0$, $\Sigma(1385)^\pm$ and $\Lambda(1520)$ resonances was observed in central A+A collisions at SPS, RHIC and LHC \rightarrow dominance of rescattering over regeneration \rightarrow consistent with existence of a long enough hadronic phase \rightarrow hadronic phase lifetime ~ 10 fm/c
- ❖ Hadronic phase affects most of observables measured in the final state (flow, correlations, yields, etc.)
- ❖ Measurements for resonances are vital to cross check the hadronic phase models
- ❖ Only models with validated hadronic phase afterburners can be used for comparison with real data to infer properties of the early partonic phase of heavy-ion collisions

Non-central heavy-ion collisions:



- ❖ Light quarks can be polarized by $|\vec{J}|$ and $|\vec{B}|$
- ❖ If vector mesons are produced via recombination their spin may align
- ❖ Quantization axis:
 - ✓ normal to the production plane (momentum of the vector meson and the beam axis)
 - ✓ normal to the event plane (impact parameter and beam axis)
- ❖ Measured as anisotropies:

NPA 1005 (2021) 121733



$$\frac{dN}{d\cos\theta} = N_0 [1 - \rho_{0,0} + \cos^2\theta (3\rho_{0,0} - 1)]$$

$\rho_{0,0}$ is a probability for vector meson to be in spin state = 0 $\rightarrow \rho_{0,0} = 1/3$ corresponds to no spin alignment

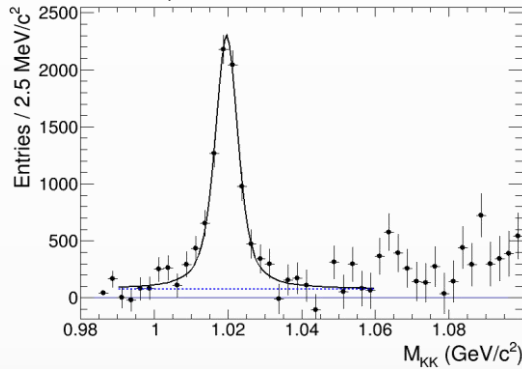
- ❖ Measurements at RHIC/LHC challenge theoretical understanding $\rightarrow \rho_{0,0}$ can depend on multiple physics mechanisms (vorticity, magnetic field, hadronization scenarios, lifetimes and masses of the particles)

BiBi@9.2 GeV (UrQMD), 10 M events \rightarrow full event/detector simulation and reconstruction

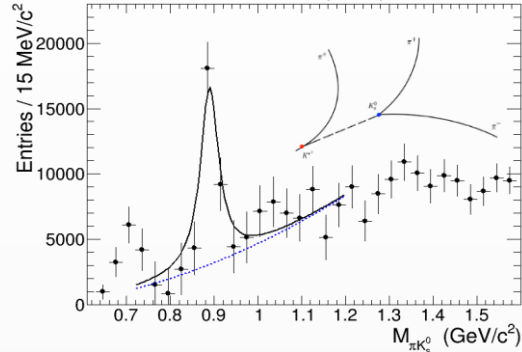
Invariant mass distributions after mixed-event background subtraction

Phys.Scripta 96 (2021) 6, 064002

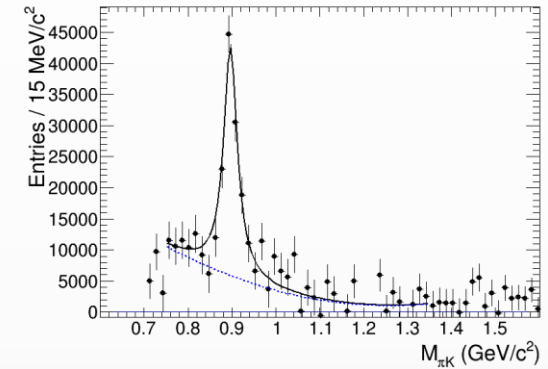
$\phi(1020) \rightarrow K^+K^-$



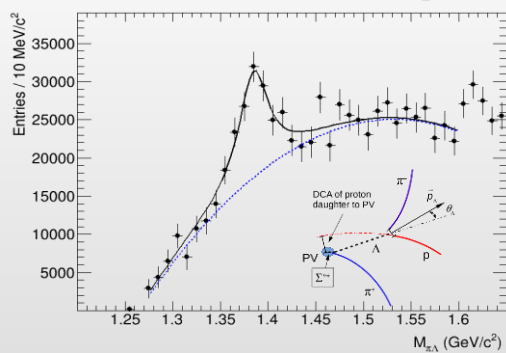
$K^*(892)^{\pm} \rightarrow \pi^{\pm}K_s (K_s \rightarrow \pi^+\pi^-)$



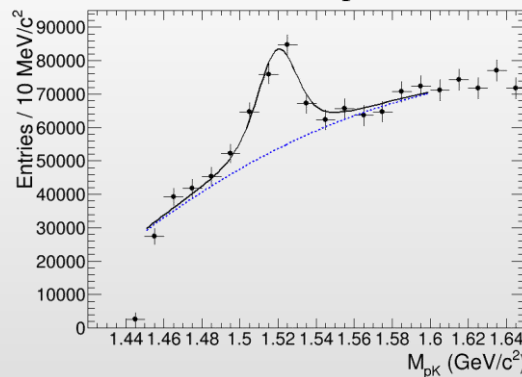
$K^*(892)^0 \rightarrow \pi^+K^-$



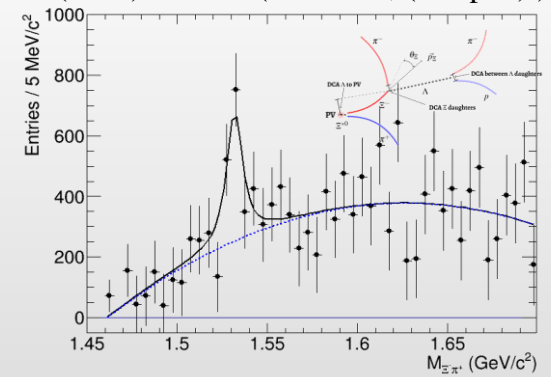
$\Sigma(1385)^{\pm} \rightarrow \pi^{\pm}\Lambda (\Lambda \rightarrow p\pi)$



$\Lambda(1520) \rightarrow pK^-$

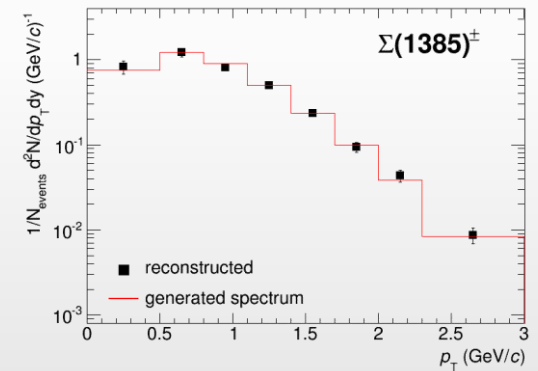
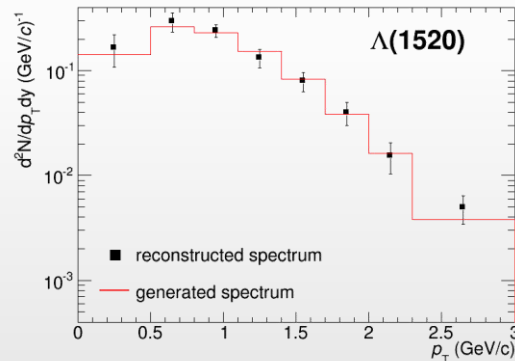
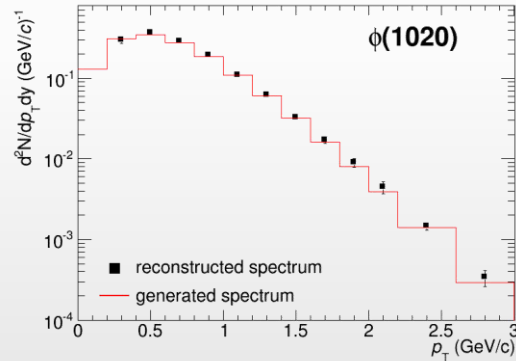
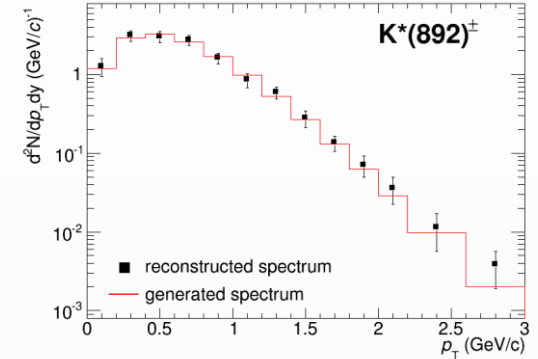
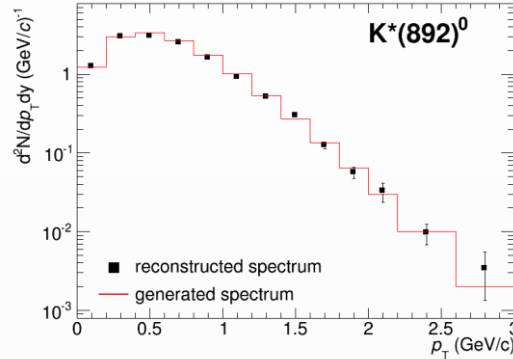
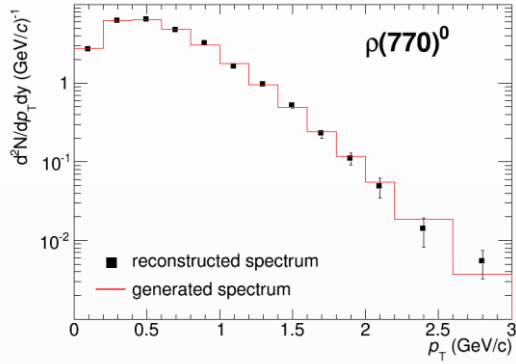


$\Xi(1530)^0 \rightarrow \pi^+\Xi^- (\Xi^- \rightarrow \Lambda\pi, (\Lambda \rightarrow p\pi))$



- ❖ MPD can reconstruct resonance signals using combined charged particle identification in TPC+TOF and secondary vertex topology selections for weakly decaying daughters

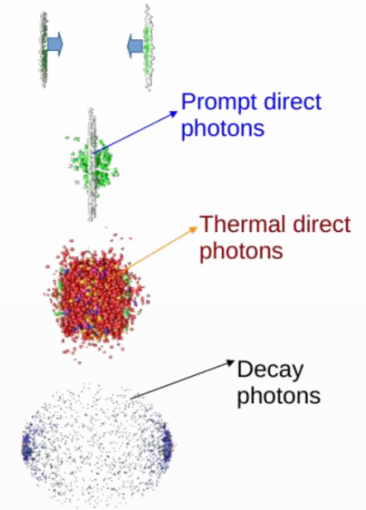
BiBi@9.2 GeV (UrQMD), 10 M events \rightarrow full event/detector simulation and reconstruction



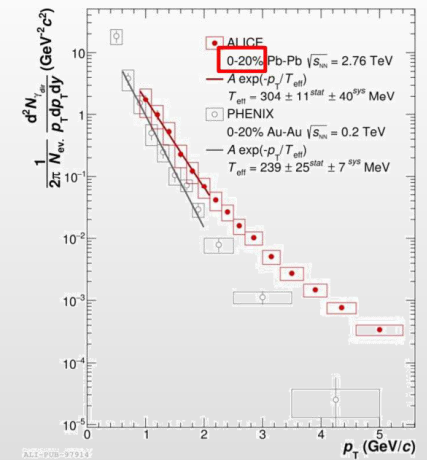
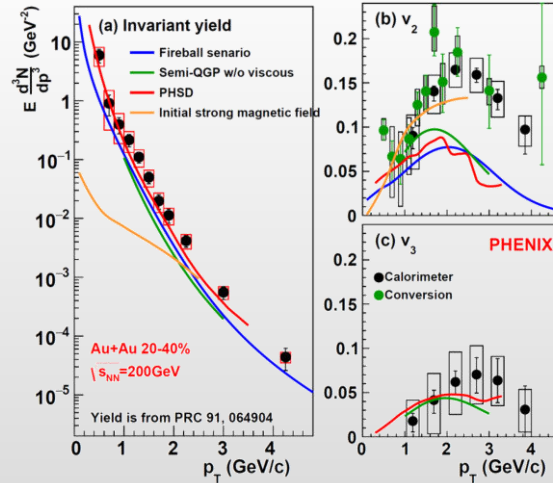
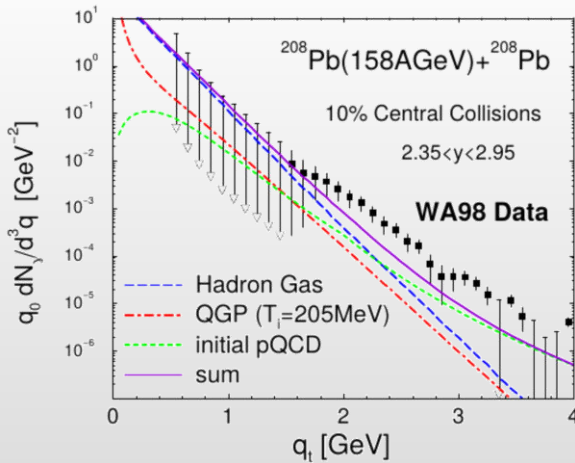
- ❖ Reconstructed spectra match the generated ones within uncertainties
- ❖ First measurements for resonances will be possible with accumulation of ~ 10 M Bi+Bi events
- ❖ Measurements are possible starting from \sim zero momentum \rightarrow sample most of the yield

Direct photons

- ❖ Direct photons – photons not from hadronic decays.
- ❖ Produced throughout the system evolution (thermal + prompt) :
 - ✓ penetrating probe
 - ✓ low-E - most direct estimation of the effective system temperature
 - ✓ high-E - hard scattering probe
- ❖ Direct photons in A-A collisions:
 - ✓ LHC, PbPb @ 2.76 and 5 TeV
 - ✓ RHIC, Au-Au(CuCu) @ 62-200 GeV
 - ✓ SPS, PbPb @ 17.2 GeV
- ❖ No measurements at NICA energies: yields and flow vs. p_T and centrality



Phys.Rev. C94 (2016) no.6, 064901



Simultaneous description of the large photon yields and flow is a challenge for theoretical models at RHIC and the LHC \rightarrow “direct photon puzzle”

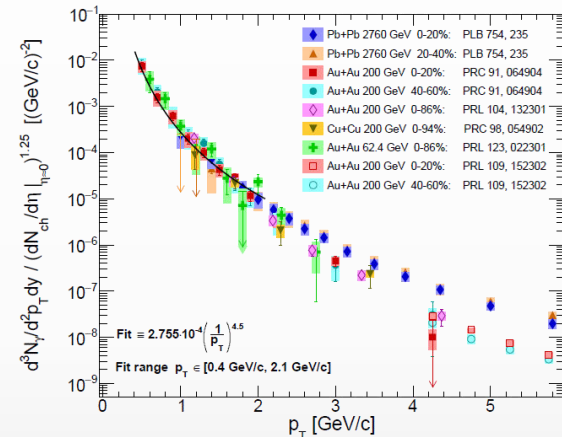
Direct photon yields at NICA

Estimation of the direct photon yields @NICA

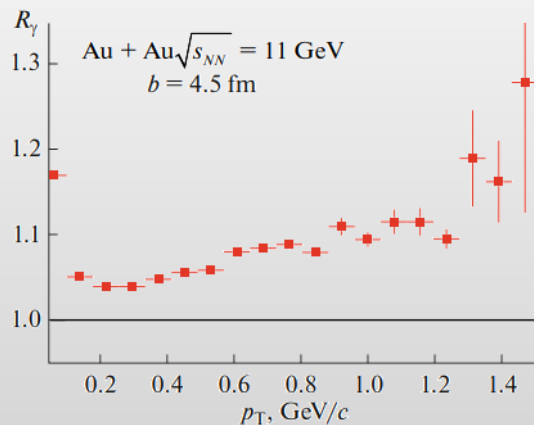
model
calculations

empirical
scaling

- ✓ UrQMD v3.4 with hybrid model (3+1D hydro, bag model EoS, hadronic rescattering and resonances within UrQMD)
- ✓ each cell have T_i, E_i, μ_i :
 - T is high – QGP phase (Peter Arnold, Guy D. Moore, Laurence G. Yaffe, JHEP 0112:009 2001)
 - T is low – HG phase (Simon Turbide, Ralf Rapp, Charles Gale, Phys.Rev.C69:014903,2004)
 - T is intermediate – mixed phase
- ✓ integrate over all cells and all time steps
- ✓ calculations reproduce hydro calculations for the SPS

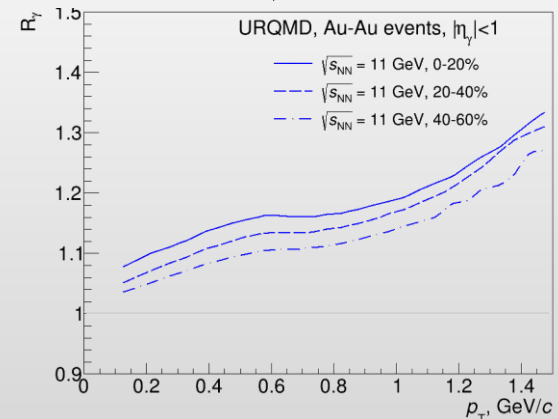


Physics of Particles and Nuclei, 2021, Vol. 52, No. 4, pp. 681–685



$$R_\gamma = \frac{\gamma_{\text{inc}}}{\gamma_{\text{decay}}} = \frac{\gamma_{\text{inc}}/\pi^0}{\gamma_{\text{decay}}/\pi^0_{\text{param}}}$$

$$\gamma_{\text{direct}} = \left(1 - \frac{1}{R_\gamma}\right) \cdot \gamma_{\text{inc}}$$

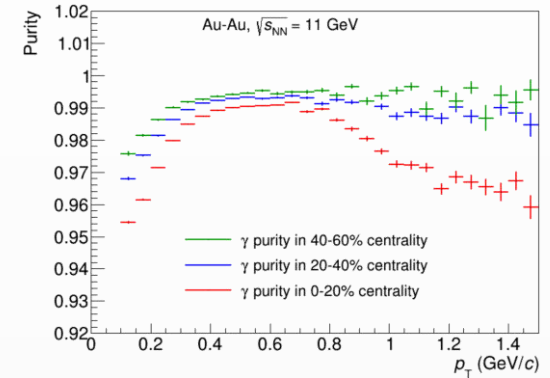
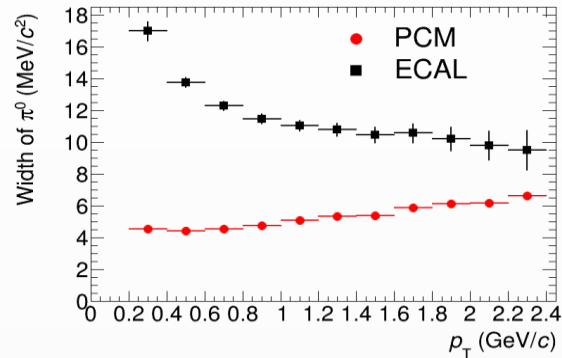
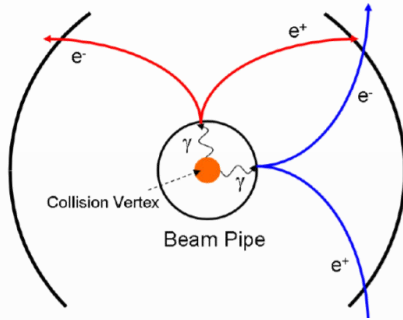


- ❖ Non-zero direct photon yields are predicted with $R_\gamma \sim 1.05 - 1.15$ and $v_2 \sim 0.5\%$ at top NICA energy

Prospects for the MPD

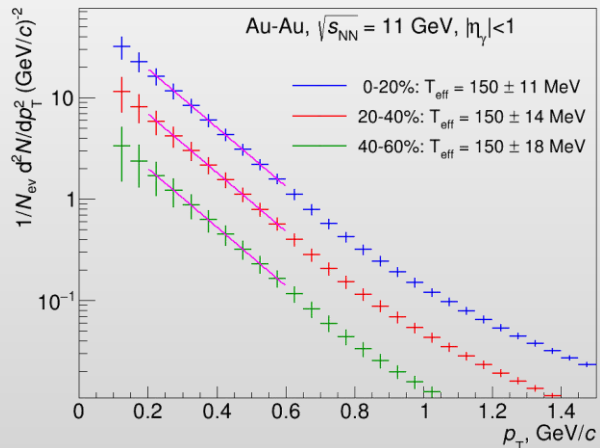
- ❖ Photons can be measured in the ECAL or in the tracking system as e^+e^- conversion pairs (PCM)

beam pipe (0.3% X_0) + inner TPC vessels (2.4% X_0)



- ❖ Main sources of systematic uncertainties for direct photons:

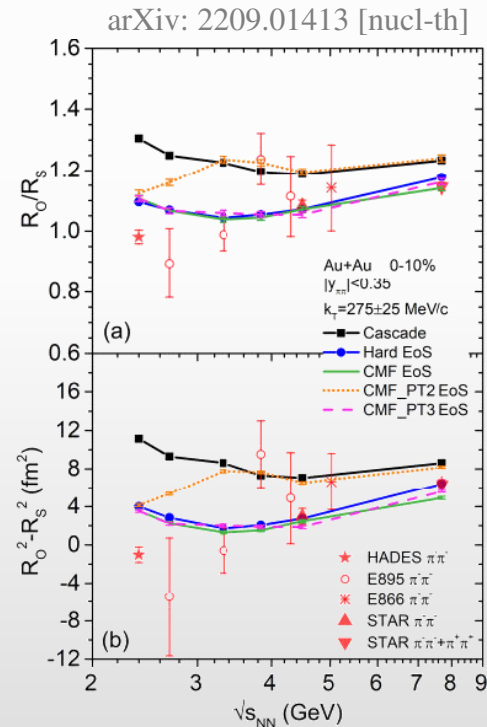
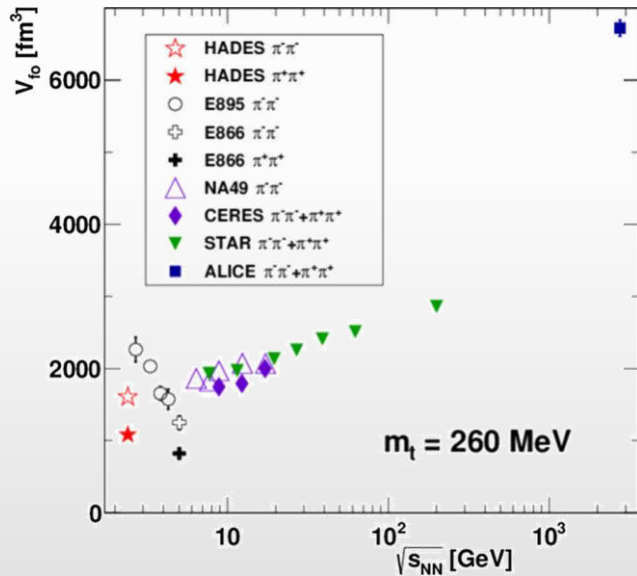
- ✓ detector material budget \rightarrow conversion probability
- ✓ π^0 reconstruction efficiency
- ✓ p_T -shapes of π^0 and η production spectra



- ✓ ECAL and PCM for photon reconstruction and measurement of neutral mesons (background)
- ✓ With $R_\gamma \sim 1.1$ and $\delta R_\gamma/R_\gamma \sim 3\%$ \rightarrow uncertainty of $T_{\text{eff}} \sim 10\%$
- ✓ Development of reconstruction techniques and estimation of needed statistics are in progress

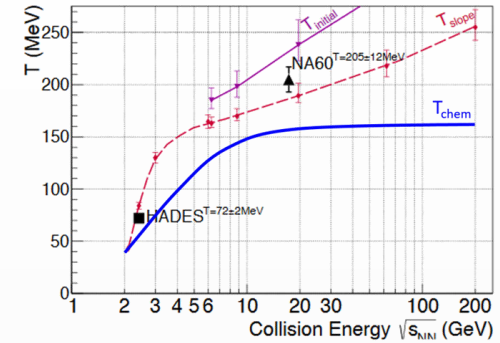
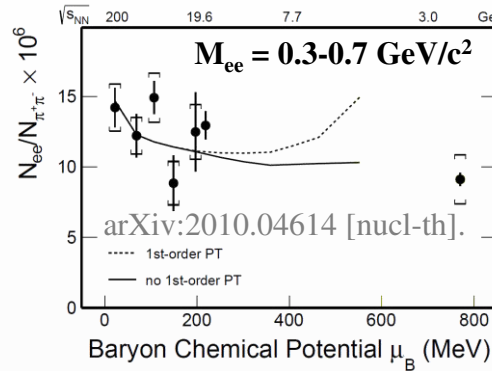
\rightarrow potentially, MPD can provide unique measurements for direct photon production in the NICA energy range

- ❖ Femtoscopy measurements:
 - ✓ size of the particle-emitting region and space-time evolution of the produced system
 - ✓ Y-N, Y-Y interaction potential (Nature 588 (2020) 7837, 232-238)
- ❖ Measurement for pions are straightforward and robust, large discovery potential in correlations for kaons and protons, as well as correlations including hyperons



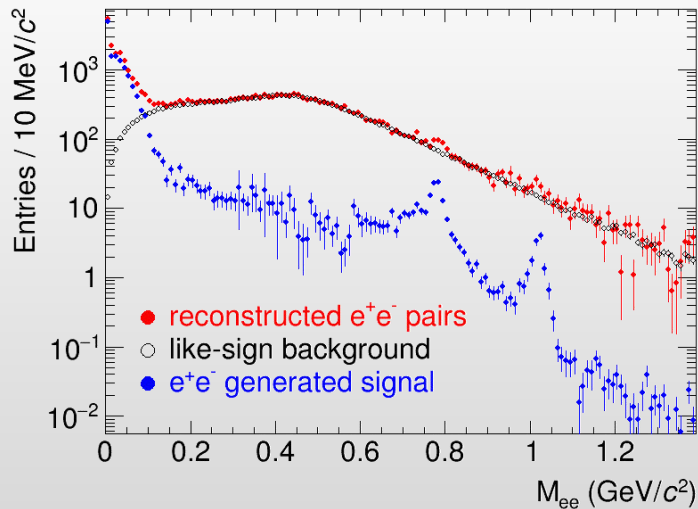
- ❖ Pion source radii are sensitive to the nature of the phase transition

- ❖ HBT measurements for identical particles
- ❖ Yield and flow of e^+e^- pairs:
 - ✓ probe deconfinement and chiral symmetry restoration
 - ✓ effective temperature



T. Galatyuk et al., *Eur. Phys. J. A* 52 (2016) 131; R. Rapp and H. v. Hess, *PLB* 753 (2016) 586
 J.Cleymans et al. 2006 *Phys. Rev. C* 73, 034905
 NA60: H. Specht, *AIP Conf. Proc.* 1322 (2010) 160; HADES: *Nature Physics* 15 (2019) 1040

BiBi@9.2 GeV (UrQMD+PHSD), 10 M events \rightarrow full event/detector simulation and reconstruction



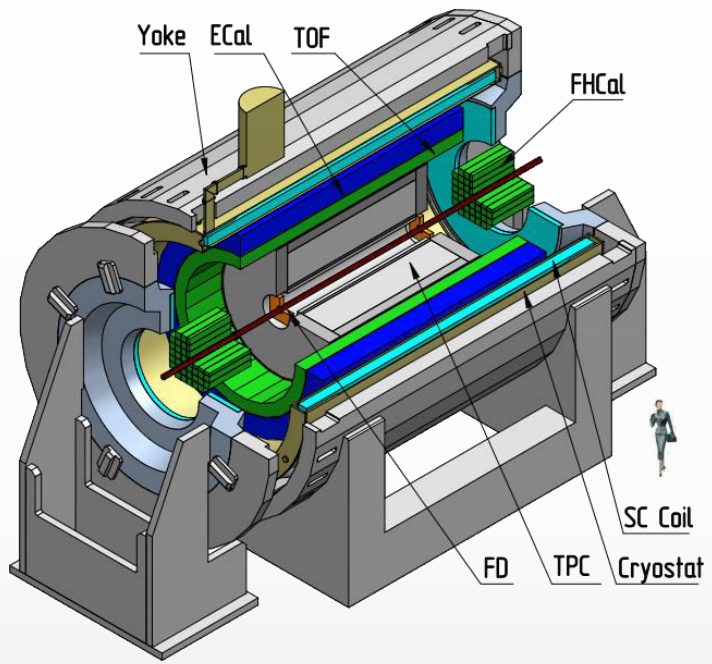
- S/B (integrated in 0.2-1.5 GeV/c²) \sim 5-10%
- Methods to improve S/B ratio with a minimal penalty for pair reconstruction are being developed
- Meaningful measurements for e^+e^- continuum and LVMs would require $\sim 10^8$ events, first observations will be possible with ~ 50 M events



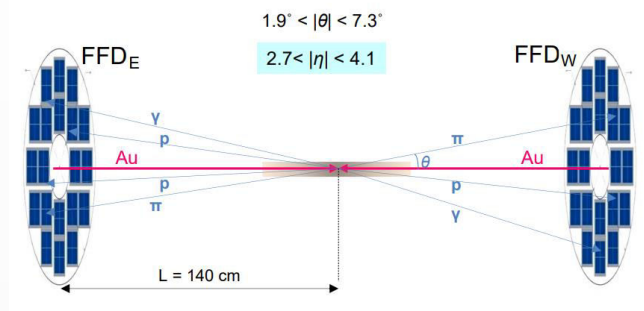
- ❖ Preparation of the MPD detector and experimental program is ongoing, all activities are continued
- ❖ All components of the MPD 1-st stage detector are in advanced state of production
- ❖ Commissioning of the MPD Stage-I detector and the first data taking with BiBi@9.2 in 2024
- ❖ Further program will be driven by the physics demands and NICA capabilities

BACKUP

Trigger system

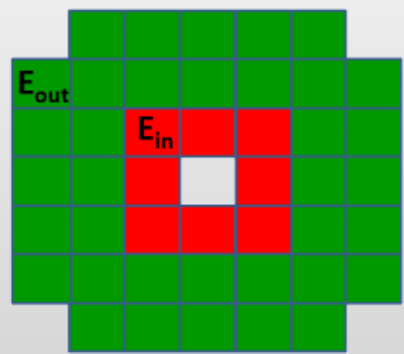


- FFD (Fast Forward Detector):
 - ✓ fast event triggering
 - ✓ T_0 for time measurements in the TOF and ECAL



- FHCAL (Forward Hadron Calorimeter) – detector for event centrality and reaction plane measurements with potential for event triggering

- MPD challenges at NICA energies:
 - ✓ low multiplicity of particles produced in heavy-ion collisions
 - ✓ particles are not ultra-relativistic (even the spectator protons)



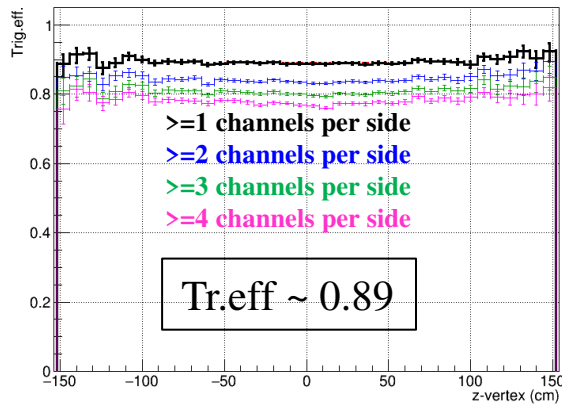
$2 < |\eta| < 5$
 $\sim 1 \times 1 \text{ m}^2$

- Forward detectors are in advanced state of production (electronics and integration)

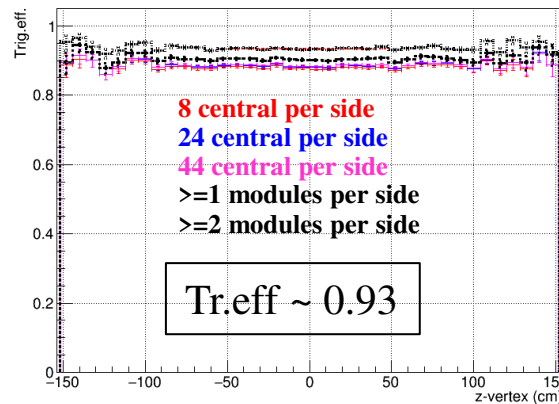
Trigger efficiency vs. z-vertex

DCM-QGSM-SMM, BiBi@9.2

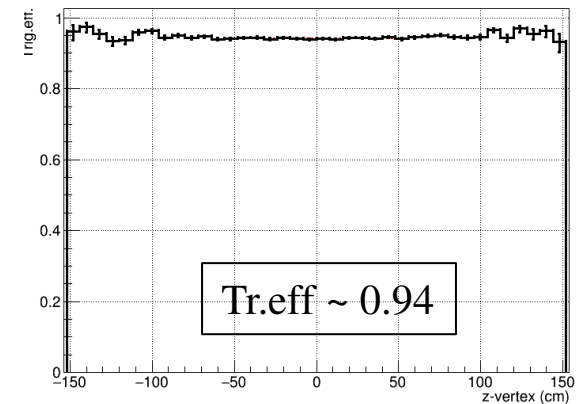
FFD trigger efficiency vs. z-vertex



FHCAL trigger efficiency vs. z-vertex

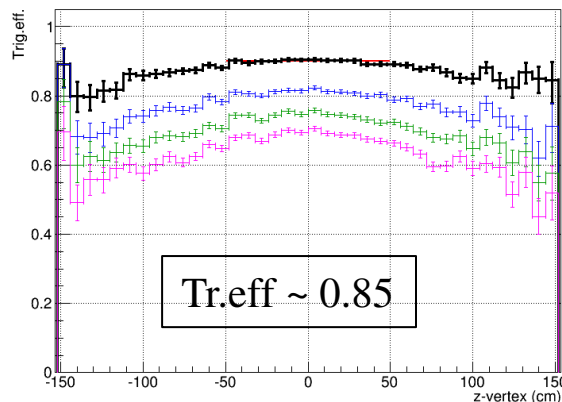


FFD||FHCAL trigger efficiency vs. z-vertex

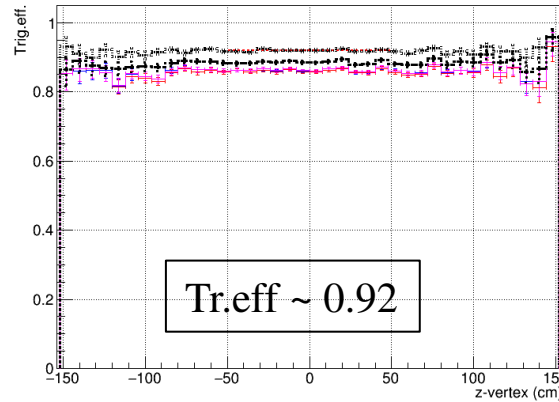


PHQMD, BiBi@9.2

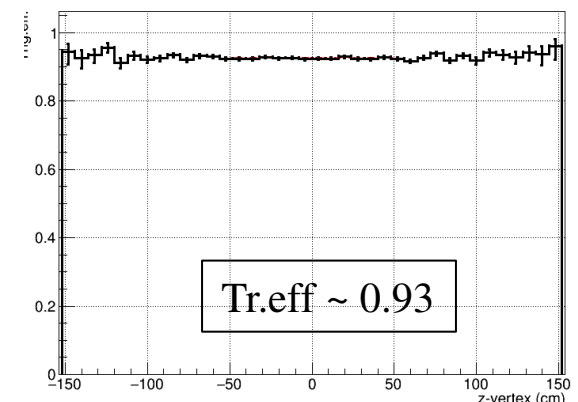
FFD trigger efficiency vs. z-vertex



FHCAL trigger efficiency vs. z-vertex



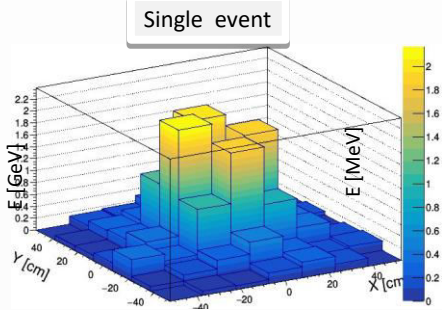
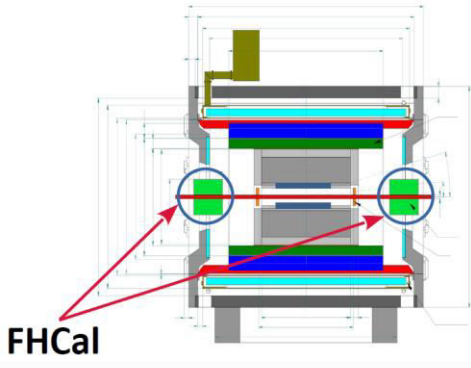
FFD||FHCAL trigger efficiency vs. z-vertex



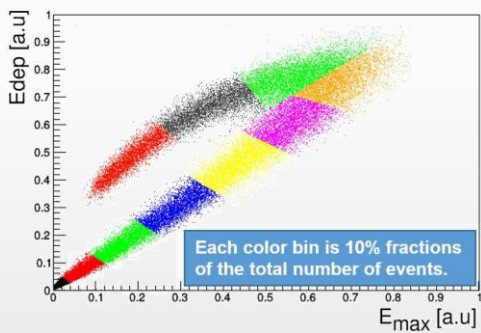
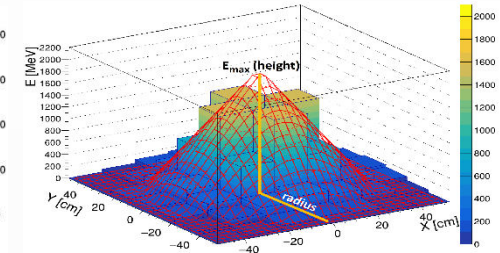
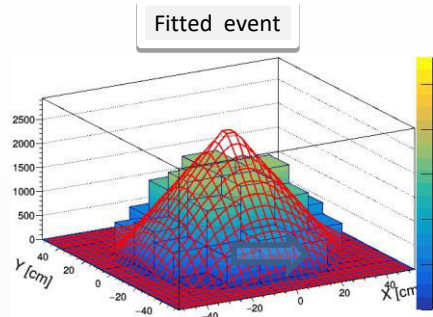
- Efficiency is 80-95% in different trigger configuration; approximately the same numbers for two generators
- FFD efficiency shows z-vertex dependence for PHQMD; FHCAL and FFD||FHCAL does not

Centrality and reaction plane by FHCAL

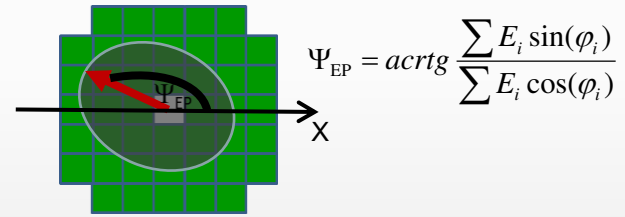
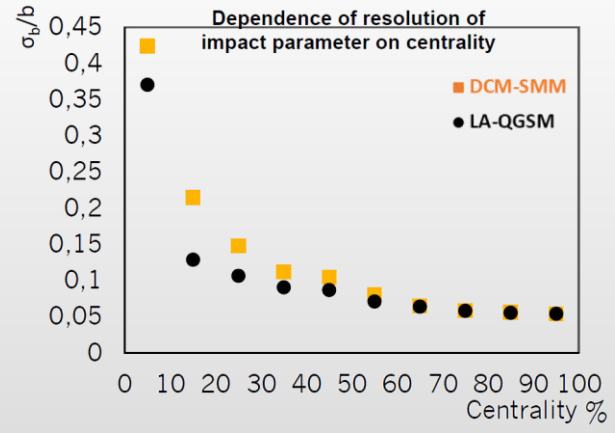
❖ FHCAL is a hadronic calorimeter, $\sim 1 \text{ m}^2$, segmentation $15 \times 15 \text{ cm}^2$, $2 < |\eta| < 5$



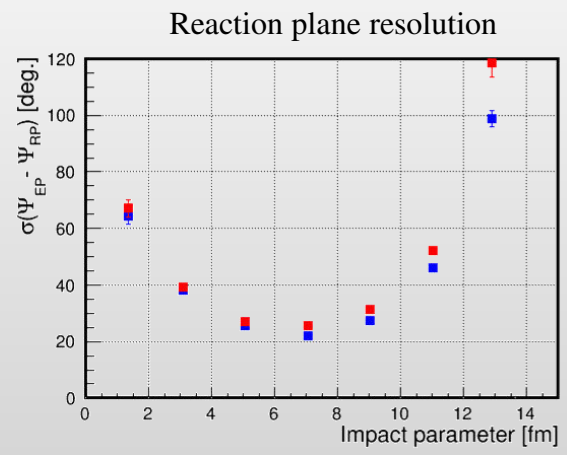
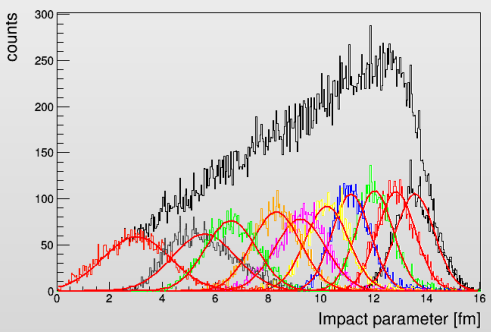
Two-dimensional fit of the energy depositions in FHCAL



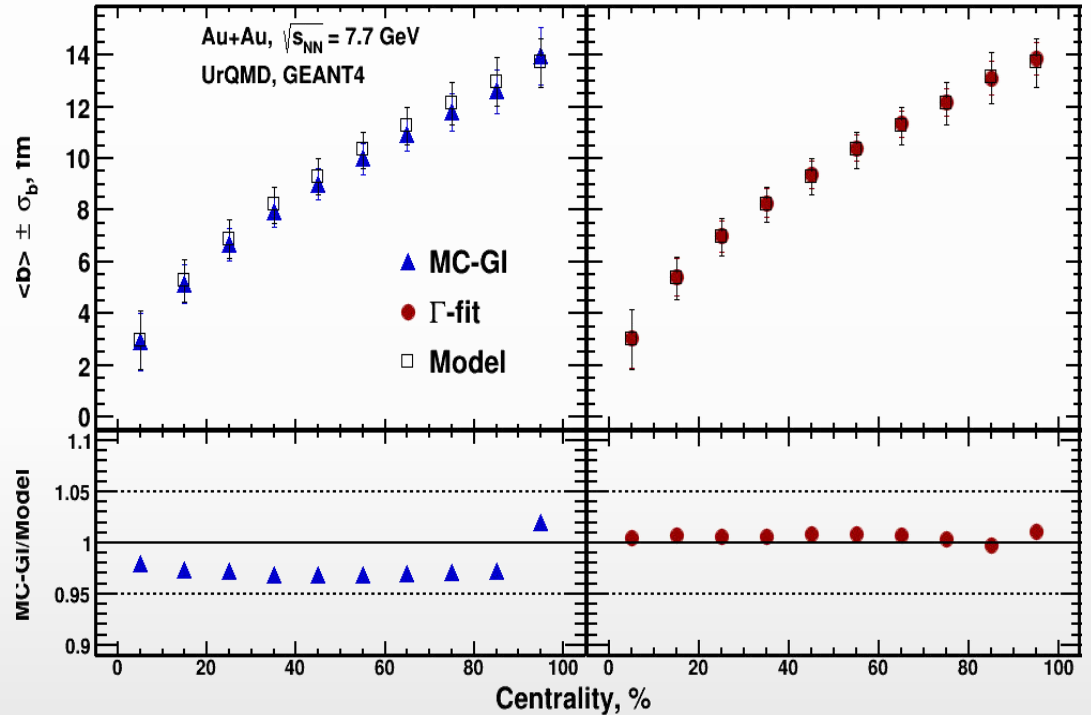
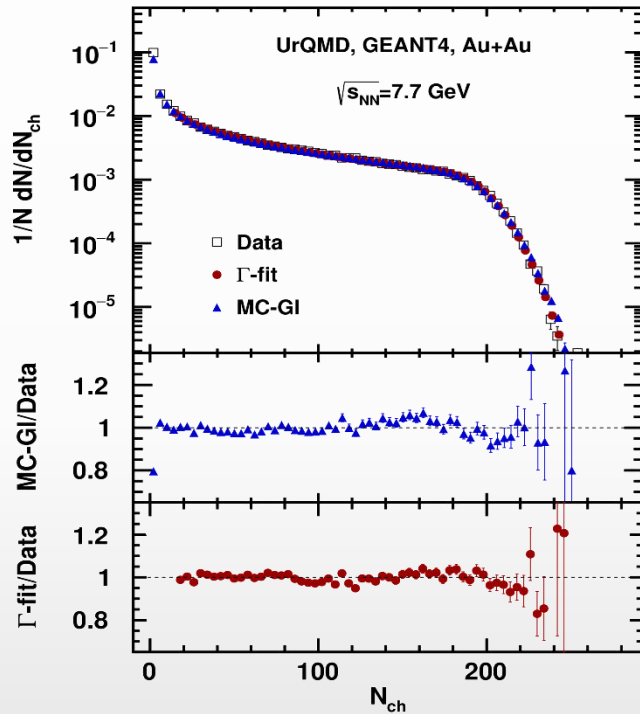
Phys.Part.Nucl. 52 (2021) 4, 578-583
AIP Conf.Proc. 2377 (2021) 1, 030015



$$\Psi_{EP} = \text{arctg} \frac{\sum E_i \sin(\varphi_i)}{\sum E_i \cos(\varphi_i)}$$



- ❖ AuAu@7.7 GeV (UrQMD), reconstructed data
- ❖ **MC Glauber (MC-GI)** and **Bayesian inversion method (Γ -fit)** methods for extraction of b



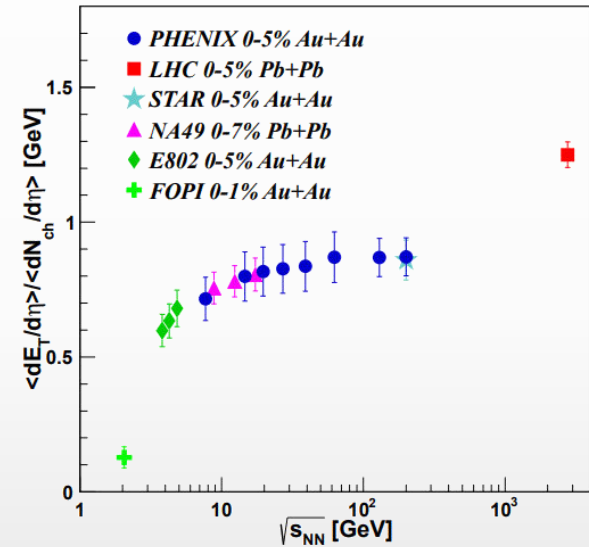
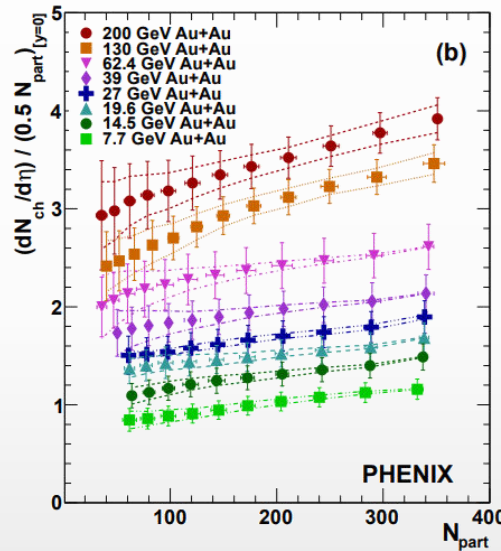
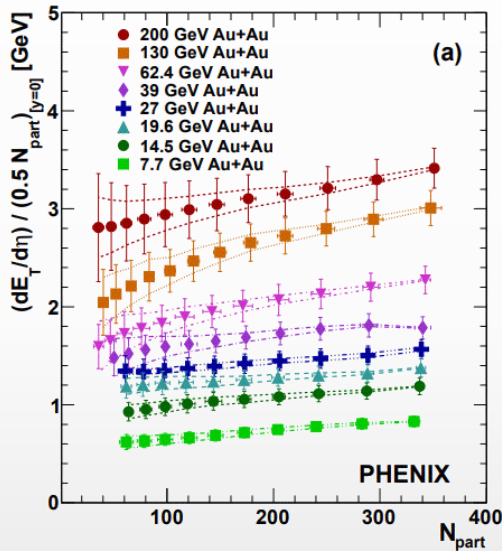
- ❖ Comparable results with PHSD and SMASH event generators at different energies \rightarrow robust method
- ❖ Centrality estimation consistent with STAR \rightarrow good for cross-checks between the experiments
- ❖ Centrality measurements are possible in a wide $|z\text{-vertex}| < 120$ cm range

[1] Centrality Determination in Heavy-ion Collisions with MPD Detector at NICA, Acta Physica Polonica B 14 (2021) 3, 503-506

[2] Relating Charged Particle Multiplicity to Impact Parameter in Heavy-Ion Collisions at NICA Energies, Particles 4 (2021) 2, 275-287

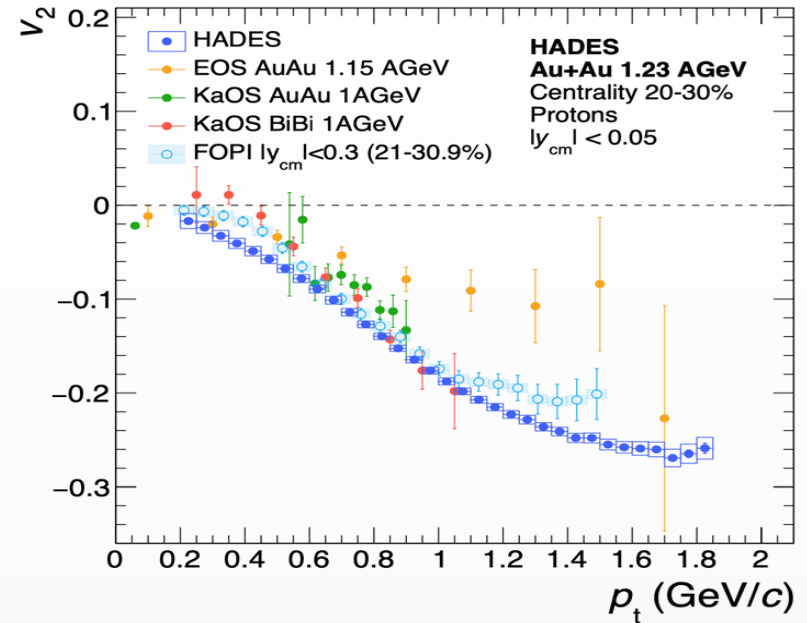
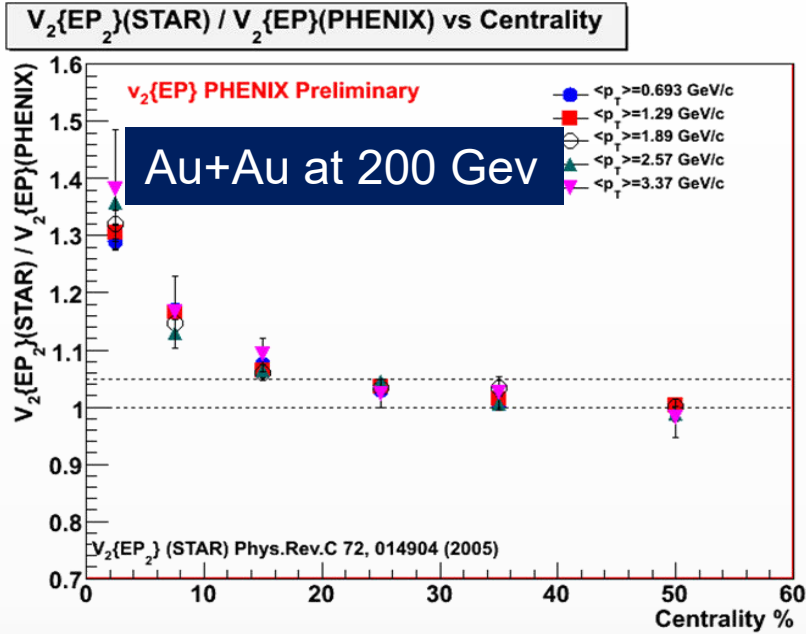
- ❖ Transverse energy and charged-particle multiplicity provide characterization of the nuclear geometry of the reaction, sensitive to dynamics of the colliding system (centrality, energy density, etc.)
- ❖ E_T/N_{ch} at NICA shows a quick increase of the average transverse mass of the produced particles

Phys.Rev.C 93 (2016) 2, 024901



- ❖ Many references for cross-checks with other experiments
- ❖ The measurements will constitute the first physics results from the MPD

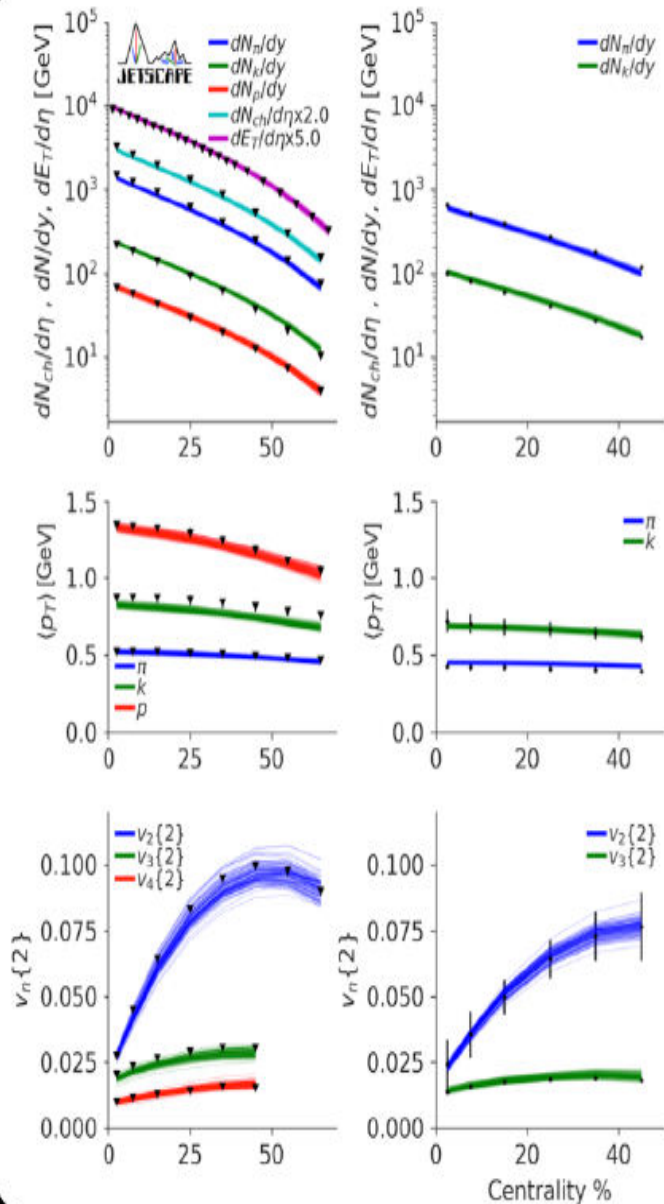
Why do we need new measurements at BM@N and MPD?



- ❖ The main source of existing systematic errors in v_n measurements is the difference between results from different experiments at the same collision energy
- ❖ A good measurement should be reproducible; in particular, it should be done in such a way that one can easily compare results from different experiments, using different detectors.

“Eliminating experimental bias in anisotropic-flow measurements of high-energy nuclear collisions”, Matthew Luzum, Jean-Yves Ollitrault, Phys.Rev. C87 (2013) 4, 044907

GLOBAL BAYESIAN CONSTRAINTS ON QGP VISCOSITY



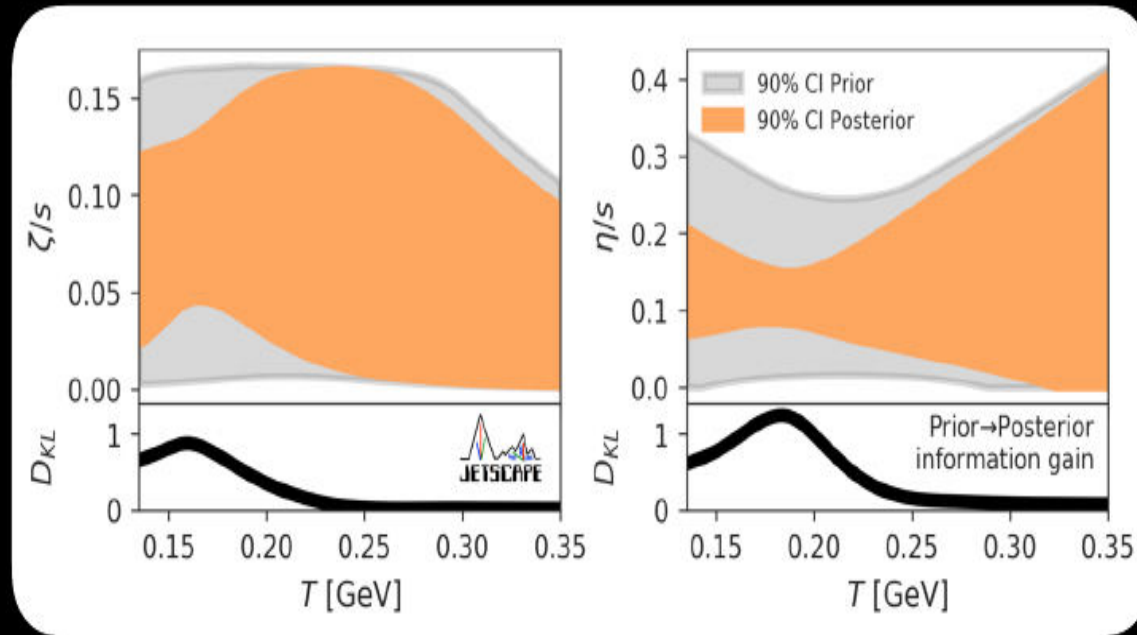
S. Pratt, E. Sangaline, P. Sorensen and H. Wang, Phys. Rev. Lett. 114, 202301 (2015)

J. E. Bernhard, J. S. Moreland, S. A. Bass, J. Liu and U. Heinz, Phys. Rev. C94, 024907 (2016)

J. E. Bernhard, J. S. Moreland and S. A. Bass, Nature Phys. 15, 1113-1117 (2019)

G. Nijs, W. Van Der Schee, U. Gürsoy and R. Snellings, Phys. Rev. Lett. 126, 202301 (2021) & Phys. Rev. C103, 054909 (2021)

D. Everett *et al.* [JETSCAPE], Phys. Rev. Lett. 126, 242301 & Phys. Rev. C103, 054904 (2021)



- Precision hadronic measurements can systematically constrain the QGP viscosity

Elliptic flow measurements using TPC: Scalar product, Event-plane

$$u_2 = \cos 2\phi + i \sin 2\phi = e^{2i\phi}$$

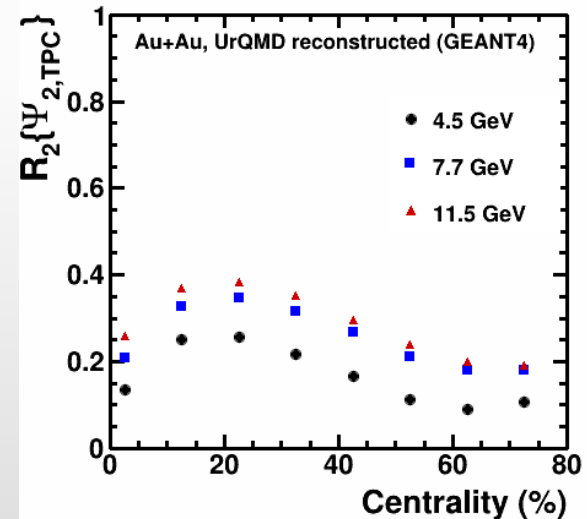
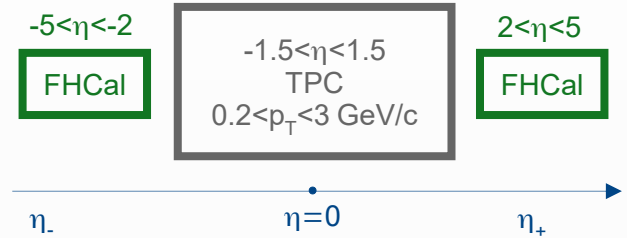
$$Q_2 = \sum_{j=1}^M \omega_j u_{2,j}, \quad \Psi_{2,\text{TPC}} = \frac{1}{2} \tan^{-1} \left(\frac{Q_{2,y}}{Q_{2,x}} \right)$$

- **Scalar product:**
$$v_2^{\text{SP}} \{Q_{2,\text{TPC}}\} = \frac{\langle u_{2,\eta\pm} Q_{2,\eta\mp}^* \rangle}{\sqrt{\langle Q_{2,\eta+} Q_{2,\eta-} \rangle}}$$

- **TPC Event-plane:**

$$v_2^{\text{EP}} \{\Psi_{2,\text{TPC}}\} = \frac{\langle \cos [2(\phi_{\eta\pm} - \Psi_{2,\eta\mp})] \rangle}{R_2^{\text{EP}} \{\Psi_{2,\text{TPC}}\}}$$

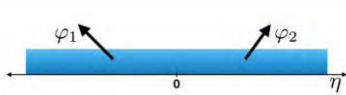
$$R_2^{\text{EP}} \{\Psi_{2,\text{TPC}}\} = \sqrt{\langle \cos [2(\Psi_{2,\eta+} - \Psi_{2,\eta-})] \rangle}$$



Vinh Ba Luong, MPD Physics Forum March 31, 2021

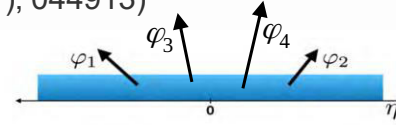
Elliptic flow measurements using TPC: Q-Cumulants

- **Standard Q-Cumulants:** (A. Bilandzic et al., Phys. Rev. C **83** (2011), 044913)



$$\langle 2 \rangle_n = \frac{|Q_n|^2 - M}{M(M-1)} \approx v_2^2 + \delta$$

$$v_2\{4\} = \sqrt[4]{2\langle\langle 2 \rangle\rangle^2 - \langle\langle 4 \rangle\rangle}$$



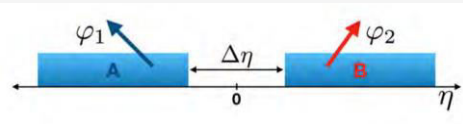
$$\langle 4 \rangle_n = \frac{[Q_n]^4 + [Q_{2n}]^2 - 2\Re[Q_{2n}Q_n^*Q_n^*] - 4(M-2)[Q_n]^2 - 2M(M-3)}{M(M-1)(M-2)(M-3)} \approx v_2^4 + 4v_2^2 + 2\delta^2$$

δ – nonflow contribution

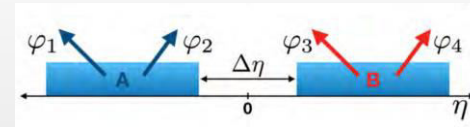
- resonance decay
- jets



- **Subevent Q-Cumulants:** (J. Jia et al., Phys. Rev. C **96** (2017), no. 3, (



$$\langle 2 \rangle_{a|b} = \frac{Q_{n,a}Q_{n,b}^*}{M_a M_b}, v_2\{2,2 - \text{sub}\} = \sqrt{\langle\langle 2 \rangle\rangle_{a|b}}$$



$$\langle 4 \rangle_{a,a|b,b} = \frac{(Q_{n,a}^2 - Q_{2n,a})(Q_{n,b}^2 - Q_{2n,b})^*}{M_a(M_a-1)M_b(M_b-1)}, v_2\{4,2 - \text{sub}\} = \sqrt[4]{2\langle\langle 2 \rangle\rangle_{a|b}^2 - \langle\langle 4 \rangle\rangle_{a,a|b,b}}$$

Note: In this presentation, all of $v_2\{2\}$ result is obtained by subevent method to suppress non-flow contribution

Sensitivity of different methods to flow fluctuations

- Elliptic flow fluctuations: $\sigma_{v_2}^2 = \langle v_2^2 \rangle - \langle v_2 \rangle^2$
- Assuming $\sigma_{v_2} \ll \langle v_2 \rangle$ and a Gaussian form for flow fluctuations
- Fluctuations enhance $v_2\{2\}$ and suppress high-order **Q-Cumulants** compared to $\langle v_2 \rangle$:
- (S. A. Voloshin, A. M. Poskanzer, and R. Snellings, Landolt-Bornstein **23** (2010), 293)

$$v_2\{2\} \approx \langle v_2 \rangle + \frac{1}{2} \frac{\sigma_{v_2}^2}{\langle v_2 \rangle} \qquad v_2\{4\} \approx v_2\{6\} \approx v_2\{8\} \approx v_2\{\text{LYZ}\} \approx \langle v_2 \rangle - \frac{1}{2} \frac{\sigma_{v_2}^2}{\langle v_2 \rangle}$$

- **TPC EP method:** (M. Luzum et al., Phys. Rev. C **87** (2013) 4, 044907)

$$\langle v_2 \rangle \leq v_2^{\text{EP}}\{\Psi_{2,\text{TPC}}\} \leq \sqrt{\langle v_2^2 \rangle} \approx \langle v_2 \rangle + \frac{1}{2} \frac{\sigma_{v_2}^2}{\langle v_2 \rangle}$$

- **Scalar product:**

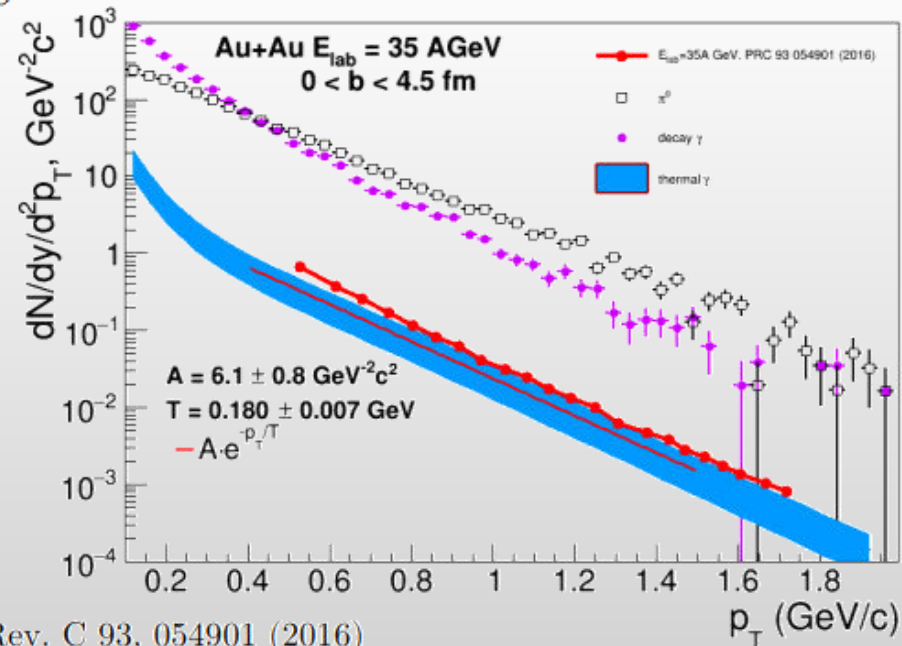
$$v_2^{\text{SP}}\{Q_{2,\text{TPC}}\} \approx \langle v_2 \rangle + \frac{1}{2} \frac{\sigma_{v_2}^2}{\langle v_2 \rangle}$$

Simulation setup

- ✓ UrQMD v3.4 with hybrid model (3+1d hydro, **bag model** EoS, hadronic rescattering and resonances within UrQMD)
- ✓ π^0 and decay photon spectrum are calculated **within the same simulation**
- ✓ impact parameter range $0 < b < 9$ fm
- ✓ In hydrodynamical evolution, for each volume we calculate thermal gamma yield based on T , energy density (e), QGP fraction, baryonic chemical potential. We integrate these yields over time (until freeze-out time) and space.
- ✓ Two extreme cases: calculate thermal gamma emission from the volume above freeze-out criterion ($e > e_{\text{freezeout}}$), or calculate for all volumes. Reality somewhere in between (all volumes interact during hydro evolution). Comparing these options one can estimate theoretical uncertainties

$$\frac{d^3 N^{\gamma, \text{therm}}}{dy d^2 k_T} = \int_{\Omega} dV dt R_{\gamma}(k, T(x), \mu(x), u(x))$$

Why simulations in PRC 93 054901 (2016) and PRC 81 044904 (2010) have almost the same yield despite ~5 times difference in energy (35 vs 158 AGeV)?



Experimental challenges in fluctuations measurements

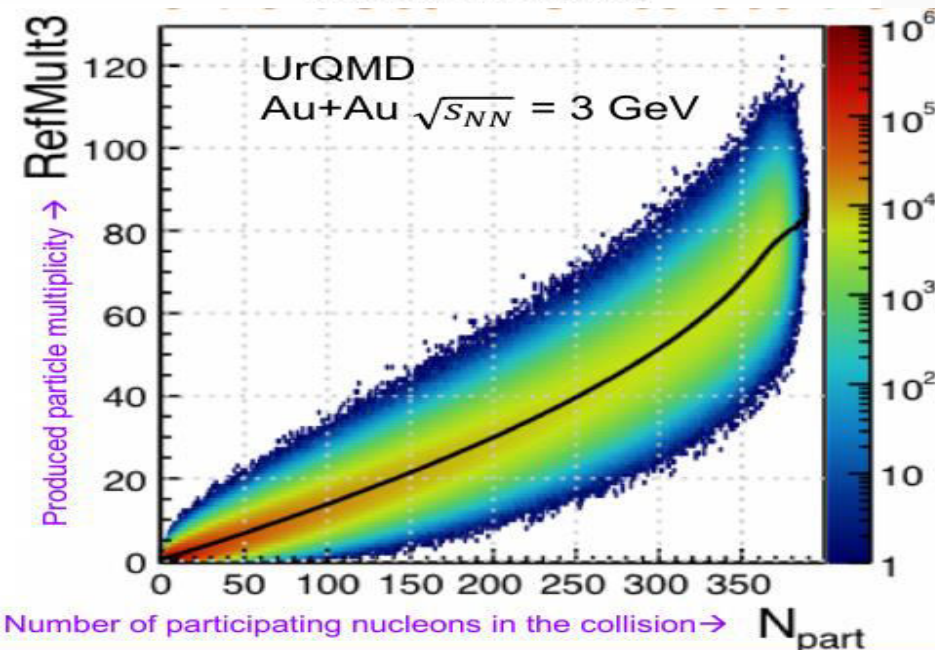
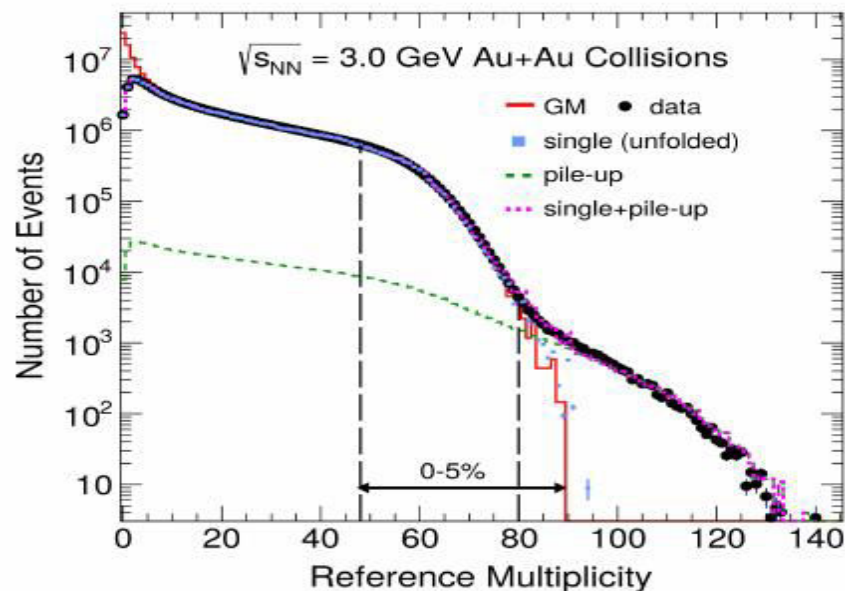
Event-by-event identification issues

- Cut based approach
- Identity method
- PSET identity method

Non-dynamical contributions

- E-by-e fluctuations of wounded nucleons
- Depends on centrality selection methods

Contributions from pileup events



Finite-Size Effects and search for CEP

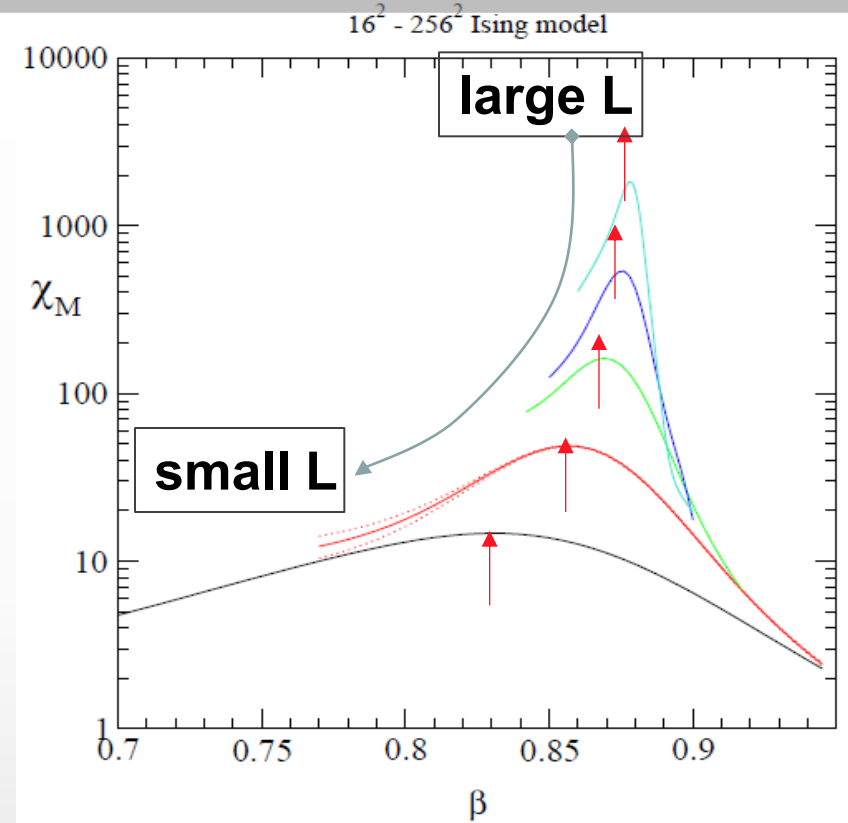
In HIC, both the size (L) and duration of formed system are finite.

Critical behavior changes with L

If the L is too small, the correlation length ξ can not be fully developed to cause a phase transition.

if the correlation length $\xi \sim |T - T_c|^{-\nu} \leq L$ the finite-size effect is not negligible and only a **pseudo-critical point, shifted from the genuine CEP, is observed.**

- ✓ Finite-size effects have a specific dependencies on size (L)
- ✓ The scaling of these dependencies give access to the CEP's location, it's critical exponents and scaling function.



Note change in peak heights positions & widths with L